

Molecular Docking and Analysis of In Silico Generated Ligands against SARS-CoV-2 Spike and Replicase Proteins

Ifeanyichukwu Okeke

Bioinformatics and Genomics Unit, Department of Pharmaceutical and Medicinal Chemistry, Afinity Laboratories and Biosciences Concerns, Nigeria

*Corresponding Author's Email: arnyic@yahoo.com

Article's History

Submitted: 18th November 2022

Accepted: 17th December 2022

Published: 21st December 2022

Abstract

Aim: The novel coronavirus also known as coronavirus disease 2019 (COVID-19), or Severe Acute Respiratory Syndrome Coronavirus 2 (SARS-CoV-2), which broke out in the latter part of the year 2019, took the entire human race unawares. This is due to its devastating health, social and economic consequences. In this study, the ability of some small molecules to interact with some SARS-CoV-2 proteins was investigated in silico for the purpose of discovering molecules which can be employed in the areas of COVID-19 diagnosis and treatment.

Methods: By way of molecular docking, a library of in silico generated ligands was docked to SARS-CoV-2 spike and replicase proteins to identify leads with propensity to bind them with high affinity. The identified leads proved to bind these proteins with stronger affinity than the native ligand aiding in their in vivo metabolic processes.

Results: It was observed that spike protein binds to its cellular receptor with binding affinity of -4.8Kcal/mol; it binds to a non-cellular analogue with -5.4, while 4twy 3BL and 5n19 D03 bind spike protein with binding affinities of -7.3Kcal/mol each. They also bind replicase protein with -8.2 and -7.2 Kcal/mol respectively. 5c8s G3A and 2d2d ENB were identified as the most suitable leads for SARS-CoV-2 spike protein detection, while 3d62 959 and 1r4l XX5 were identified as leads with most suitable druglikeness against SARS-CoV-2. These findings indicate that the identified ligands can preferentially displace or inhibit binding of the viral proteins to their native endogenous ligands and that both cellular attachment through spike and ACE2 interaction, and viral replication process can both be inhibited by using just one of the substances identified. This study is part of efforts in finding non recombinant nucleic acid solutions to SARS-CoV-2 diagnosis and treatment. If these findings are implemented, they can enhance efficient detection of the virus antigens from biological samples.

Conclusion: Identifying molecules that can interact with SARS-CoV-2 proteins could optimize diagnostic and therapeutic care for patients infected with the virus.

Recommendation: Based on the study, 5c8s G3A and 2d2d ENB were identified as the most suitable leads that are favorably disposed for SARS-CoV-2 spike protein detection from biological samples. Also, 3d62 959 and 1r4l XX5 were identified as leads with most suitable drug likeness against SARS-CoV-2 based on the filters from SwissADME and Molinspiration cheminformatics and therefore deserve further in vitro and in vivo evaluations.

Keywords: *In silico, molecular docking, COVID-19, SARS-CoV-2, druglikeness.*

INTRODUCTION

Background of the Study

The outbreak of the novel coronavirus also known as coronavirus disease 2019 (COVID-19), or Severe Acute Respiratory Syndrome Coronavirus 2 (SARS-CoV-2) [1] in the last part of the year 2019 took the entire human race unawares with its devastating health, social and economic consequences [2]. Since the outbreak, scientists all over the world have swung into action, researching in various disciplines to find solutions to contain the virus. Among the factors limiting the effort in containing the virus especially in underdeveloped and developing countries of the world are the issues of diagnosis and treatment. Effective diagnosis and isolation of infected persons is one of the key non pharmaceutical means to contain the spread of the virus [3],[4]. Currently, the only valid test for COVID-19 is the nucleic acid amplification test (NAAT) such as real-time reverse-transcription polymerase chain reaction (rRT-PCR) [5]. This test is not readily available and affordable especially to the people in the under developed and developing countries of the world hence making access to COVID-19 test difficult in these areas [6]. To effectively control and manage any emerging, reemerging and novel diseases, early detection and characterization is very important [7].

Molecular interactions between proteins driving activities of SARS-CoV-2 and exogenous smaller molecules (ligands) which are able to bring about structural modification following occupation of the binding sites of the viral proteins thereby altering their biological functions are considered in this study as a way to enhance research in the aspects of diagnosis and treatment for the novel disease. Findings have shown that the interaction between ligands and the protein receptors which induce conformational changes in the proteins can bring about alteration in the thermodynamic stability of proteins rather than their mechanical stability with formation of new complexes that affect the activities of that particular protein [8]. These smaller molecules or ligands also known as drugs tend to find their ways into the binding pockets of the receptors molecule. The interaction which can be likened to an enzyme-inhibitor interaction which can be a competitive one whereby a native ligand is inhibited from binding to the receptor in preference for the exogenous one depending on their binding affinities and conditions that enhance it [9]. This particular concept of molecular interaction can be utilized to identify lead compounds which can be applied in laboratory detection and treatment of COVID-19.

From the foregoing, two gene products from SARS-CoV-2: the spike protein and the replicase protein were docked to their ligands as generated from the PDB (rcsb.org) to identify leads that can serve as diagnostic and therapeutic agents directly or after some possible structural optimization. The outcome of the findings indicate that most of the ligands can bind the replicase protein thereby inhibiting viral replication, while many others can bind spike protein thereby inhibiting viral attachment to their receptors in the host cell. Some of the ligands also have the ability to bind both spike and replicase proteins with much greater binding affinity than that with which the cell receptors bind them.

In this study, the reliability of in silico prediction that has been widely applied in preliminary drug discovery strategy was applied [10], [11], [12], [13] to:

1. Dock a library of computer generated ligands to SARS-CoV-2 spike and replicase proteins in order to identify leads with maximum hits with the proteins;

2. Analyze the interacting residues of the proteins with the best leads identified; and
3. Study drug suitability of the identified ligands with the best hit.

The interactions observed could also be exploited in the study of suitable biochemical diagnostic alternative to SARS-CoV-2 or COVID-19 nucleic acid amplification test (NAAT), such as real-time reverse-transcription polymerase chain reaction (rRT-PCR). SARS-CoV-2 is a highly contagious respiratory pathogen infecting humans with a very rapid spreading rate [14], [15], causing most common symptoms such as fever, dry cough and tiredness, and less common symptoms such as aches and pains, sore throat, diarrhea, conjunctivitis, headache, loss of taste or smell and skin rash or discoloration of fingers or toes. Serious symptoms may include difficulty breathing or shortness of breath, chest pain or pressure, loss of speech or movement [16], [17]. A recent report from John Hopkins University [18] indicates that latest global total cases as at January 15, 2021 stood at 93,620,509 confirmed cases with daily new cases of 746,642. The mucus membrane lining the nose, mouth and eye until lately are the entry points for the virus into the vascular networks and subsequent invasion of cells of various organs such as the nervous system lungs, heart and many others [19], [20], [21], [22]. Once into the vascular networks, entry of COVID-19 into the erythrocytes is mediated by anion exchange membrane band3 protein in its tetrameric molecular structure [23].

SARS-CoV-2 structurally has four proteins: spike (S), membrane (M), envelope (E) and nucleocapsid (N) proteins. The spike protein is responsible for attachment to the host's cellular receptor [24]. In this study, one structural (the spike protein) and one nonstructural (replicase) proteins were considered in studying the interaction of the viral proteins with some of their ligands. Attachment and fusion of SARS-CoV-2 to the host's cell receptor - angiotensin converting enzyme 2 (ACE 2) through a series of process that will not be illustrated here is facilitated by the spike protein [25], [26], [27] [28]. The expression of the S protein in some coronaviruses by an infected cell can also mediate fusion of the infected cell with adjacent uninfected cells leading to formation of multinucleated cells or syncytia. This has been considered as a strategy to allow viruses to spread directly between cells thereby avoiding virus-neutralizing antibodies [29], [30], [31].

The envelope protein (E) is an integral membrane protein involved in many activities that have to do with the life cycle of the virus such as budding, packaging, envelope formation and pathogenesis. It also functions as an ion-channelling viroporin and facilitates interactions between other coronavirus proteins and host cell proteins [32]. The E protein is richly expressed inside the infected cell during replication cycle but only a little amount of it is incorporated into virion envelope [33] while majority are deposited at the point of intracellular trafficking such as the endoplasmic reticulum, Golgi apparatus and ERGIC where it carries out the fuctions of viral packaging and budding [34].

The membrane protein (M) is the most abundant of all the structural proteins. It is regarded as the central organizer because of its role in interacting with the rest of the coronavirus structural proteins to bring about formation of virion envelope and stabilization of the N protein-RNA complex (nucleocapsid) which ultimately promotes completion of viral assembly [35] [36] [37] [38]. The primary mechanisms that direct coronavirus RNA synthesis and processing are situated within the nonstructural proteins nsp7 to nsp16. These are cleavage products of two large replicase polyproteins translated from the coronavirus genome [39].

The nucleocapsid (N) has the ability to bind coronavirus RNA genome to constitute the nucleocapsid [40] Apart from being involved with processes relating to viral genome, the N protein is also involved in coronavirus replication activity and response of the host cell to infection by the virus [41]. The replicase, though an accessory and nonstructural protein (nsp), is indispensable in the replication cycle of the N protein (a structural protein). The resolution of the structure of the replicase protein (nsp9) suggests that the protein comprises a single β -barrel with a fold previously unseen in single domain proteins. The fold superficially resembles an OB-fold with a C-terminal extension and is related to both of the two subdomains of SARS-CoV 3C-like protease (which belongs to the serine protease superfamily). The nsp9 has presumably evolved from a protease. The crystal structure suggests that the protein is dimeric [42].

MATERIALS AND METHODS

Materials

Compounds Used

The protein data bank (PDB) structures of the receptors used: spike (PDB ID: 2ghv) and replicase (PDB ID: 1uw7 (nsp9)) proteins in their prepared forms using Discovery Studio visualize v20.1.0.19295 is shown in figure 1. Structures of some of the ligand ions used are shown in figures 2 and 3.

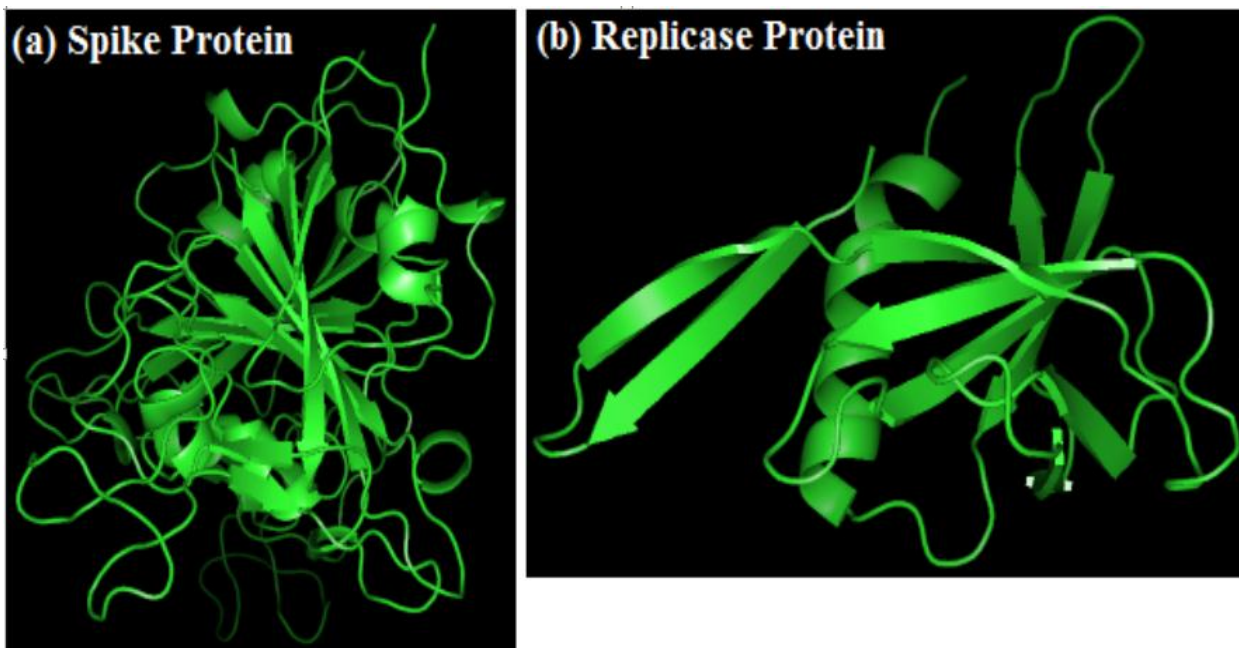


Figure 1: PDB structures of SARS-CoV-2 spike and replicase proteins

Structures of some of the ligands used are shown in figures 2 and 3.

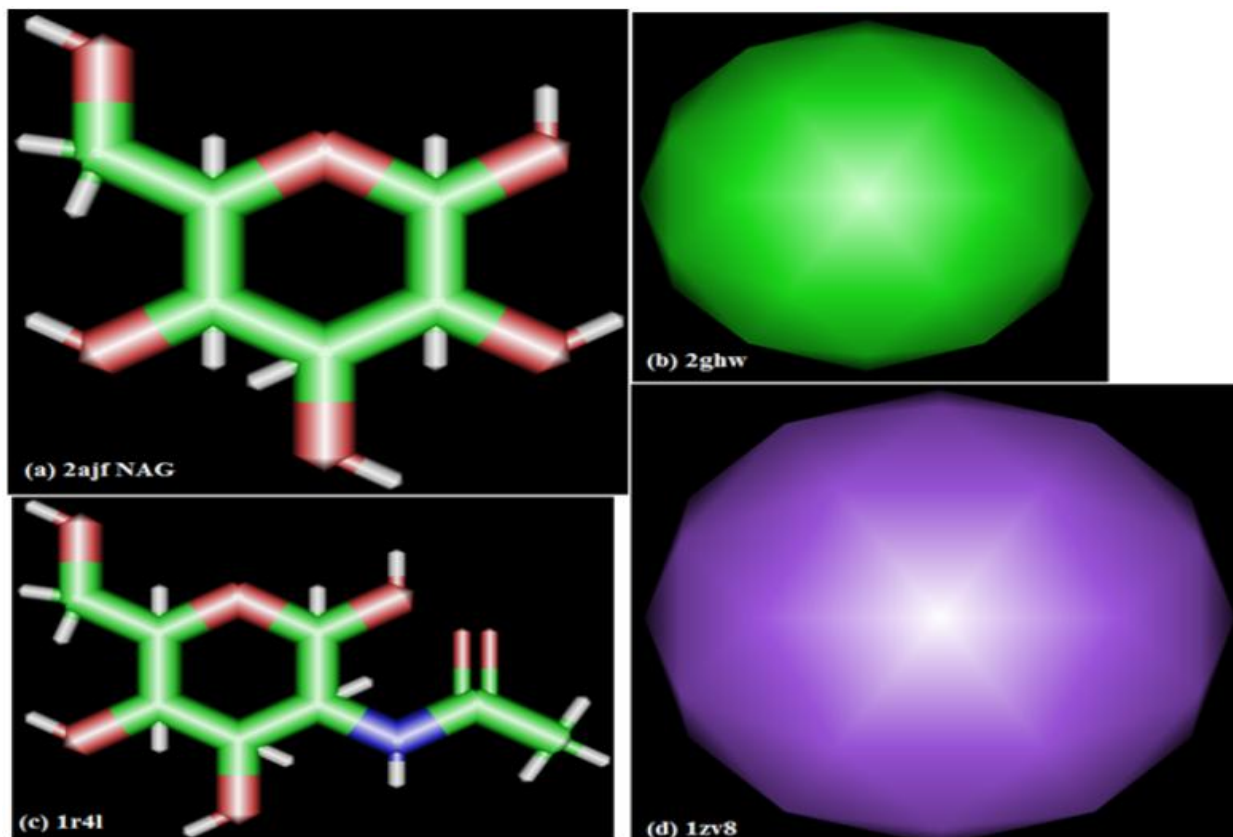


Figure 2: Images of the sdf formats of the spike protein ligands

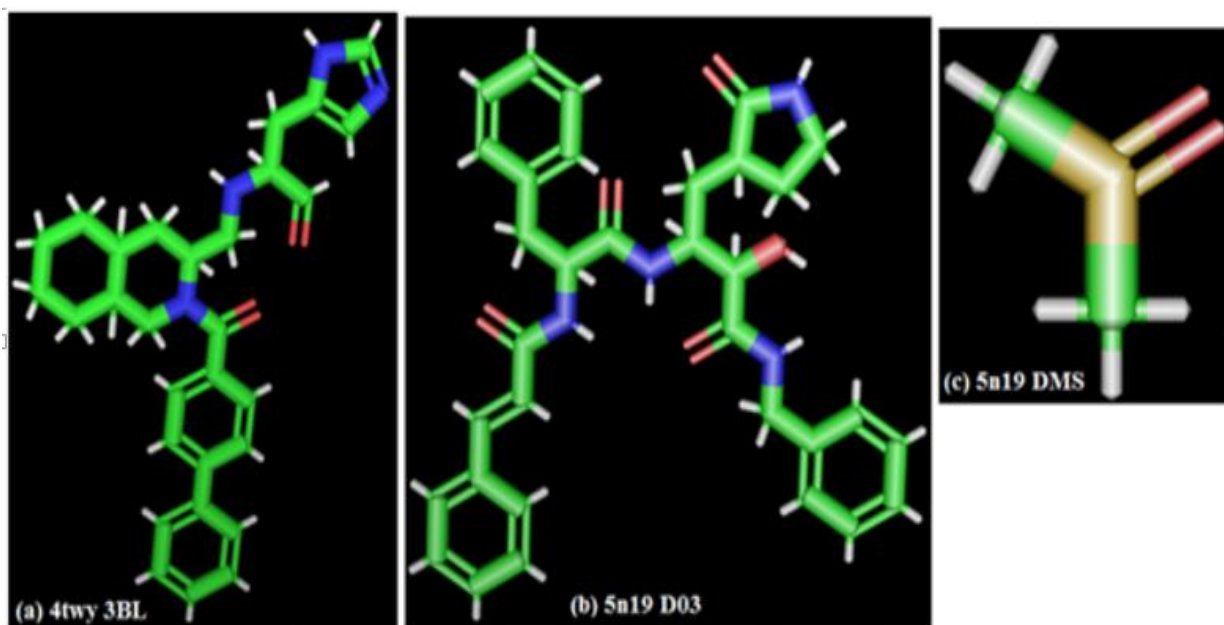


Figure 3: Images of the sdf formats of the replicase protein ligands

Hardware and Software

This work was carried out on windows 8.1 Pro with processor: Intel® Core (TM) i5 CPU M 520 @ 2.40GHz having installed memory (RAM): 4.00GB (3.86 GB usable) on system type: 64 bit operating system although 32-bit Windows Vista operating system also work well. PyRx docking software version 0.8 for Windows (<http://pyrx.sourceforge.net>) was used for molecular docking. PyRx is open source software to perform virtual screening. It is a combination of several softwares such as AutoDock Vina, AutoDock 4.2, Mayavi, Open Babel, etc. PyRx uses Vina and AutoDock 4.2 as docking softwares. In this study, AutoDock Vina [43] was used. Discovery studio (Discovery Studio: v20.1.0.19295), Pymol (Pymol stereo 3D quad buffer) and ICM Browser (Molsoft MolBrowser 3.8-7d) were used to examine structural properties and study binding interactions between receptor residues and the ligands.

Databases and Applications

The chemical structures of the receptors (2ghv and 1uw7 (nsp9) and those of their ligands were downloaded from protein data bank (rcsb.org) and PubChem (<https://pubchem.ncbi.nlm.nih.gov/>). Canonical SMILES and other information about the ligands and the receptor were extracted from PubChem.

Methods

Retrieval of Macromolecule

The structures of the receptors: spike and replicase proteins were retrieved by searching in the protein data bank (PDB) (rcsb.org/structure/); downloaded, and saved as PDB format in figure 4 [44], [45].

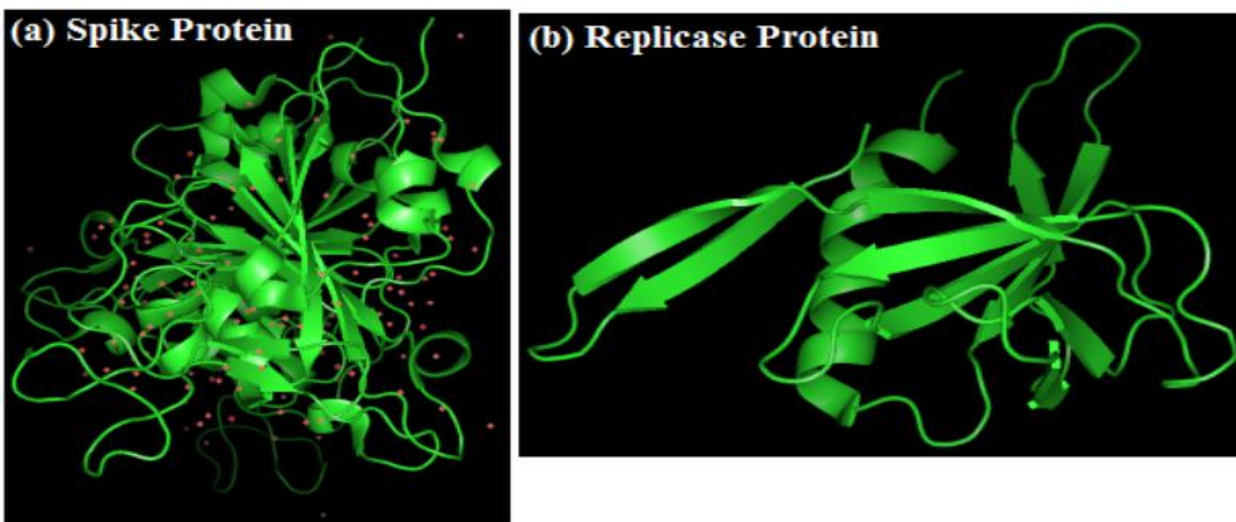


Figure 4: Images of raw PDB structures of spike and replicase

Retrieval of Liands

Molecules constituting the ligands screened (table 1) are the ligands for SARS-CoV-2 spike and replicase proteins and were extracted from rcsb.org as Excel files. Their ideal sdf formats (figures 2 and 3) were downloaded from PubChem.

Table 1: List of some of the ligands targeting SARS-CoV-2 spike and replicase proteins

| PDB_ID | Chain ID | Ligand | Ligand Formula | Ligand MW | Ligand Name |
|--------------|----------|--------|--------------------|-----------|---|
| 5C8S | B, D | G3A | C20 H27 N10 O17 P3 | 772.406 | GUANOSINE-P3-ADENOSINE-5',5'-TRIPHOSPHATE |
| 2ALV | A | CY6 | C29 H42 N4 O7 | 558.666 | N-((3S,6R)-6-((S,E)-4-ETHOXYSACRONYL-1-((S)-2-OXOPYRROLIDIN-3-YL)BUT-3-EN-2-YLCARBAMOYL)-2,9-DIMETHYL-4-OXODEC-8-EN-3-YL)-5-METHYLISOXAZOLE-3-CARBOXAMIDE |
| 2D2D | A, B | ENB | C29 H42 N4 O7 | 558.666 | ETHYL (2E,4S)-4-[((2R)-2-{{N-(TERT-BUTOXYCARBONYL)-L-VALYL]AMINO}-2-PHENYLETHANOYL)AMINO]-5-[(3S)-2-OXOPYRROLIDIN-3-YL]PENT-2-ENOATE |
| 2GX4 | A | NOL | C32 H50 N4 O7 | 602.762 | N-[(BENZYLOXY)CARBONYL]-O-(TERT-BUTYL)-L-THREONYL-3-CYCLOHEXYL-N-[(1S)-2-HYDROXY-1-[(3S)-2-OXOPYRROLIDIN-3-YL]METHYL]ETHYL]-L-ALANINAMIDE |
| 3R24 | A | SAM | C15 H22 N6 O5 S | 398.437 | S-ADENOSYLMETHIONINE |
| 1R42 ACE2 | A | NAG | C8 H15 N O6 | 221.208 | N-ACETYL-D-GLUCOSAMINE |
| 1R4L ACE2 | A | XX5 | C19 H23 Cl2 N3 O4 | 428.31 | (S,S)-2-{{1-CARBOXY-2-[3-(3,5-DICHLORO-BENZYL)-3H-IMIDAZOL-4-YL]ETHYLAMINO}-4-METHYL-PENTANOIC ACID |
| 4TWY | A | 3BL | C29 H34 N4 O2 | 470.606 | (2S)-2-{{[(3S,4aR,8aS)-2-(biphenyl-4-ylcarbonyl)decahydroisoquinolin-3-yl]methyl}amino}-3-(1H-imidazol-5-yl)propanal |
| 3D62 | A | 959 | C11 H13 N O3 | 207.226 | benzyl (2-oxopropyl)carbamate |

Target Preparation and Docking Process

The x-ray structures of the receptors (2ghv and 1uw7 (nsp9)) were downloaded from protein data bank (rcsb.org), hetatoms were removed using discovery studio and resaved (figure 1). The input

ligand files were also prepared for virtual screening by minimizing their energies and converting them to PDBQT file format when they were imported into PyRx software as chemical table file (SDF). The library of the ligands were docked into the active sites of 2ghv and 1uw7 (nsp9) in the PyRx platform using Amber Van der Waals in the active box of 16 x 15 x 17. Vina search space centre X:4.6276, Y:41.5295, Z:8.2772 and dimensions (Angstrom) X:59.9591, Y:44.6474, Z:25.0000, with a total of 200 steps. Autodock Vina took each ligand and bonded its different conformations to the macromolecules (2ghv and 1uw7 (nsp9)) separately to get the binding energies in different orientations of each ligand. Each ligand has nine different binding orientations starting from 0 to 8.

Validation of Docking Process

Docking was repeated three times on the same system specifications for the purpose of process validation and all returned minimal variation ($P<0.01$ data not shown) in uff energy, binding energy and RMSD values in the two receptors.

Binding Analysis

Discovery studio (Discovery Studio: v20.1.0.19295), Pymol (Pymol stereo 3D quad buffer) and ICM Browser (Molsoft MolBrowser 3.8-7d) were all used to visualize and analyze binding interactions between residues of the receptor molecules and the ligands.

RESULTS AND DISCUSSION

Analysis of Docking Result

A library of the ligands belonging to the SARS-CoV-2 spike and replicase proteins were docked to their binding pockets in the receptors. Compounds in the library demonstrated good binding affinity with many having higher binding affinity to the spike protein than angiotensin converting enzyme 2 (ACE2), its native (cellular) ligand (tables 2a and 2b). Analysis was restricted to 10 structures with binding energy -4.8Kcal/mol and lower. The highest binding affinity recorded in the screening is -7.3 and -8.2 Kcal/mol for spike and replicase proteins respectively with 1r4l NAG (ACE2) as the reference molecule for comparing extent of interaction between spike protein and ligands. Given the same ligand, replicase protein generally shows higher binding affinity than spike protein implying higher tendency to interact with the ligands.

Table 2a: Binding affinities of some ligands to spike protein from autodock output

| S/No. | Ligand | Target | Binding Energy Kcal/mol |
|--------------|----------------------------------|---------------|--------------------------------|
| 1 | 4twy 3BL_118729211_uff_E=905.56 | 2ghv | -7.3 |
| 2 | 5n19 D03_137349146_uff_E=800.16 | 2ghv | -7.3 |
| 3 | 5c8s G3A_135450590_uff_E=2309.40 | 2ghv | -6.8 |
| 4 | 2alv CY6_10062715_uff_E=878.66 | 2ghv | -6.8 |
| 5 | 1wof I12_15959287_uff_E=811.58 | 2ghv | -6.5 |
| 6 | 2d2d ENB_23304231_uff_E=676.52 | 2ghv | -6.4 |
| 7 | 2gx4 NOL_11844232_uff_E=996.29 | 2ghv | -6.3 |

| | | | |
|----|-------------------------------|------|------|
| 8 | 3r24 SAM_34755_uff_E=839.60 | 2ghv | -6.3 |
| 9 | 3d62 959_22747857_uff_E=96.68 | 2ghv | -5.9 |
| 10 | 1r4l XX5_448281_uff_E=661.41 | 2ghv | -5.4 |
| 11 | 2v6n XP1_12092_uff_E=103.00 | 2ghv | -4.8 |
| 12 | 1r4l NAG_24139_uff_E=431.68 | 2ghv | -4.8 |

Table 2b: Binding affinities of some ligands to replicase protein from autodock output.

| Ligand | Target | Binding Energy |
|----------------------------------|-------------|----------------|
| 4twy 3BL_118729211_uff_E=905.56 | 1uw7_(nsp9) | -8.2 |
| 5n19 D03_137349146_uff_E=800.16 | 1uw7_(nsp9) | -7.2 |
| 2gx4 NOL_11844232_uff_E=996.29 | 1uw7_(nsp9) | -6.7 |
| 2alv CY6_10062715_uff_E=942.65 | 1uw7_(nsp9) | -6.6 |
| 2d2d ENB_23304231_uff_E=699.26 | 1uw7_(nsp9) | -6.5 |
| 1wof I12_15959287_uff_E=878.61 | 1uw7_(nsp9) | -6.4 |
| 3r24 SAM_34755_uff_E=839.60 | 1uw7_(nsp9) | -6.2 |
| 3d62 959_22747857_uff_E=96.68 | 1uw7_(nsp9) | -5.9 |
| 5c8s G3A_135450590_uff_E=2281.20 | 1uw7_(nsp9) | -5.8 |

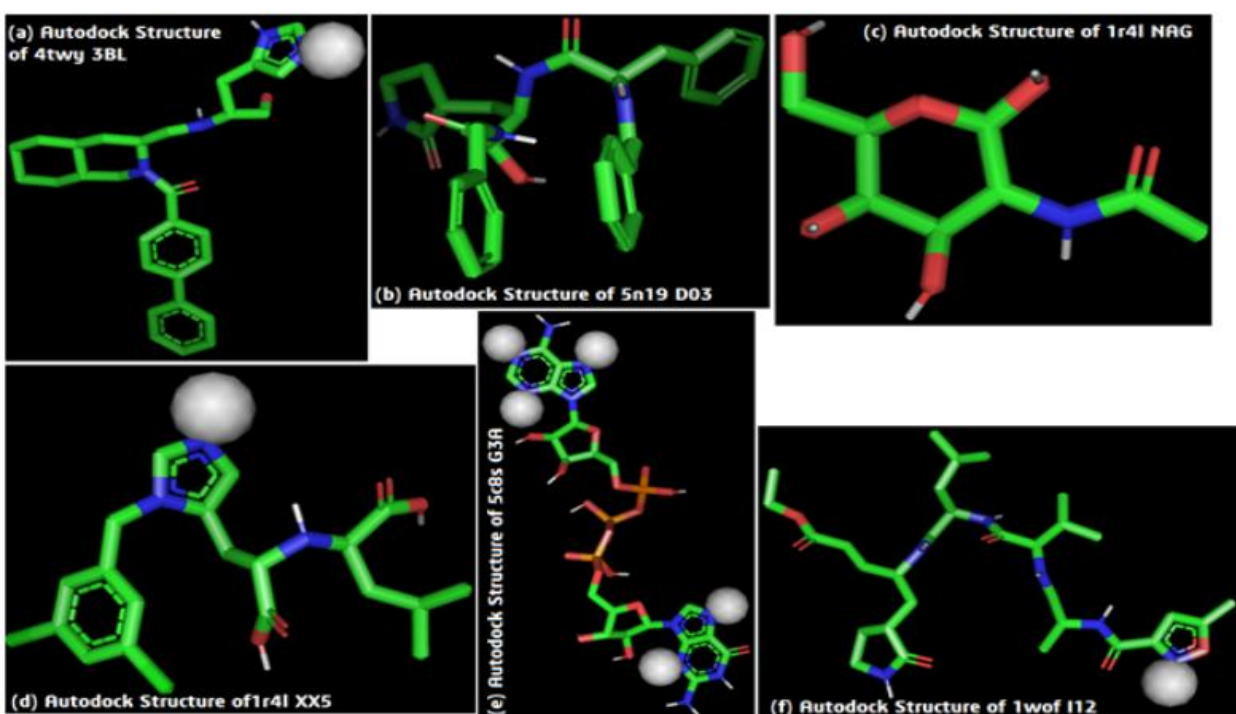


Figure 5: Images of Autodock structures of some spike protein ligand-receptor complexes

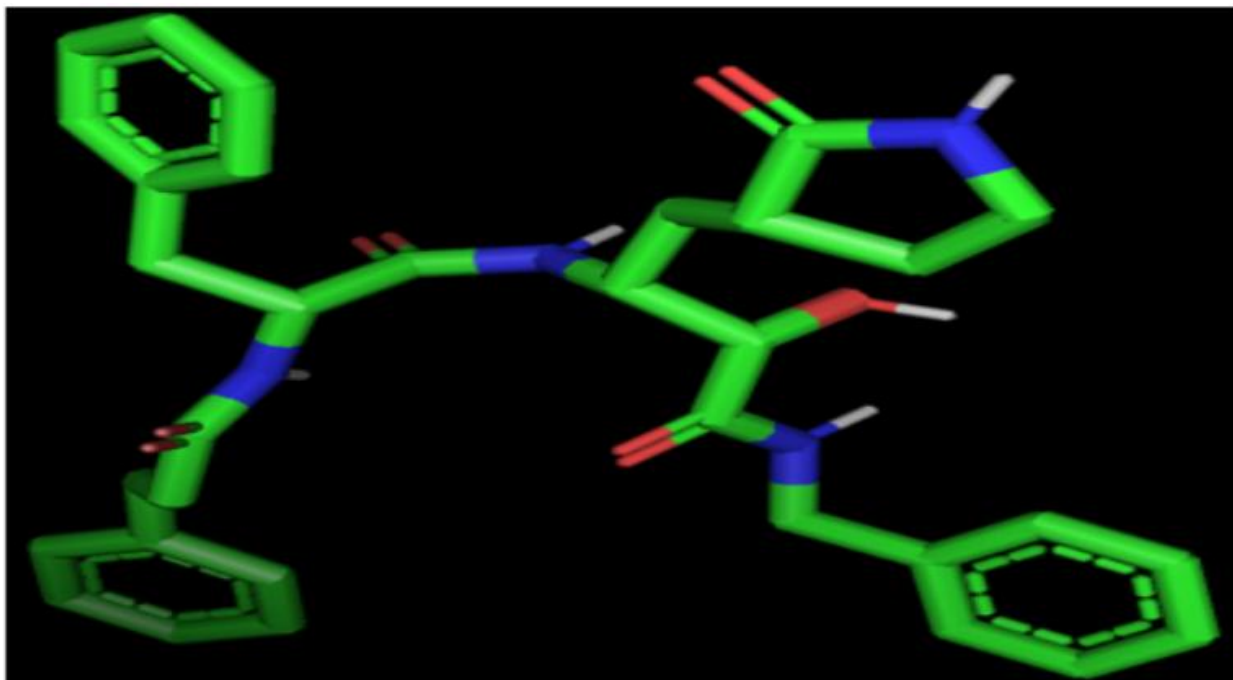


Figure 6: Autodock structure of 5n19 DO3 in association with replicase

Analysis of Kinds of Binding Interactions seen between Ligands and Receptor Residues

Here are the various types of interactions between the ligands and the residues of the spike protein receptor within the binding pocket. It was observed that the interactions are predominantly non covalent in nature typical of those for maintaining 3D structures of large molecules such as proteins and nucleic acids [46], [47]. These interactions suggest that both the ligands and the receptor are large biological molecules which specifically but transiently bind to one another to bring about biological and pharmacological responses as the case may be.

Van der Waals

These are relatively weak electric forces that attract neutral molecules. These forces can be seen in the complex formed between molecules of 4twy 3BL, 5n19 D03, 5c8s G3A, 1r4l XX5, 3d62 959 and 1r4l NAG and the receptor residues (figures 7a-f).

Unfavorable Bumps

Different schools of thought have different explanation for this type of interaction. While some believe that this type of interaction arose because the model is not a perfect imitation of the real structure [48], others [49] believe that they are due to unstable and maximum torsional strain. Melesina Jelena [50] opined that unfavorable interactions in molecular docking do not necessarily mean that the compounds are not good inhibitors. Some factors may have played some roles during the interaction and such factors may be:

- Protein flexibility is not taken into account in commonly used docking protocols so compounds might fit due to induced fit effect. In order to avoid this event, they suggested docking to several protein conformations or induced fit docking.

- The ‘right’ binding mode mode of the inhibitor might not be returned by the docking programme. For example, due to insufficient conformational sampling, or not top-scored by the used scoring function. To avoid the pitfalls of analyzing a non relevant binding mode, re-scoring sometimes helps.
- Compound might have unexpected mode of action or binding site.
- Other effects (such as solvent, entropy, target interaction partners) that are poorly accounted for during docking might play crucial roles in activity in giving rise to unfavorable bumps as seen in the interaction between 4twy 3BL, 5n19 D03, 5c8sG3A, 1r4l XX5, 3d62 959 and 1r4l NAG with the receptor residues. All the ligands analized exhibited this type of interaction (figures 7a-g).

Pi (π) Lone pair

A form of non-covalent interaction usually associated with electron cloud of aromatic ring capable of interacting with other groups such as sulfur, alkyl, stacked or lone pair [50] 4twy 3BL (figure 7a) exhibited this type of interaction among other bonds types with SARS-CoV-2 spike protein. Pi-Pi Stacked was exhibited by 4twy 3BL and 5n19 D03. It was formed due to high polarizability of aromatic rings leading to dispersive interactions of nucleobases such as in DNA [51], Pi-Alkyl seen in 4twy 3BL, 5n19 D03, 5c8s G3A and 1r4l XX5, while Pi-Sulfur was seen with 5n19 D03.

Unfavorable (or punished contact)

This is the contribution from all heavy atom contacts between ligands and the molecules included in the binding site setup. It measures the complementarities between ligand and binding site by punishing different types of heavy atom’s contact considering that inter atom distance less than 5.5Å. An *Unfavorable Acceptor-Acceptor* was seen in 5n19 D03. *Unfavorable Donor-Donor* was seen in 5c8s G3A and 1r4l XX5. All these unfavorable interactions involve hydrogen bond donor [52].

Conventional Hydrogen Bond

This is considered the most favorable (or rewarded contact) with the highest level of complementarities between binding site and ligand. An interaction whereby different kinds of heavy atom contacts are rewarded as seen in interaction between 5c8s G3A, 2alv CY6, 2d2d ENB and 1r4l NAG with the receptor [53]. Carbon-Hydrogen Bond is common among organic compounds. It is a form of covalent interaction where a carbon shares its outer valence electron with up to four hydrogen atoms. This bond confers more strength to the complex formed than van der Waals forces [54].

Alkyl

An interaction between electron groups of any alkyl group and ligands as exhibited by 1r4l XX5 in figure 7d.

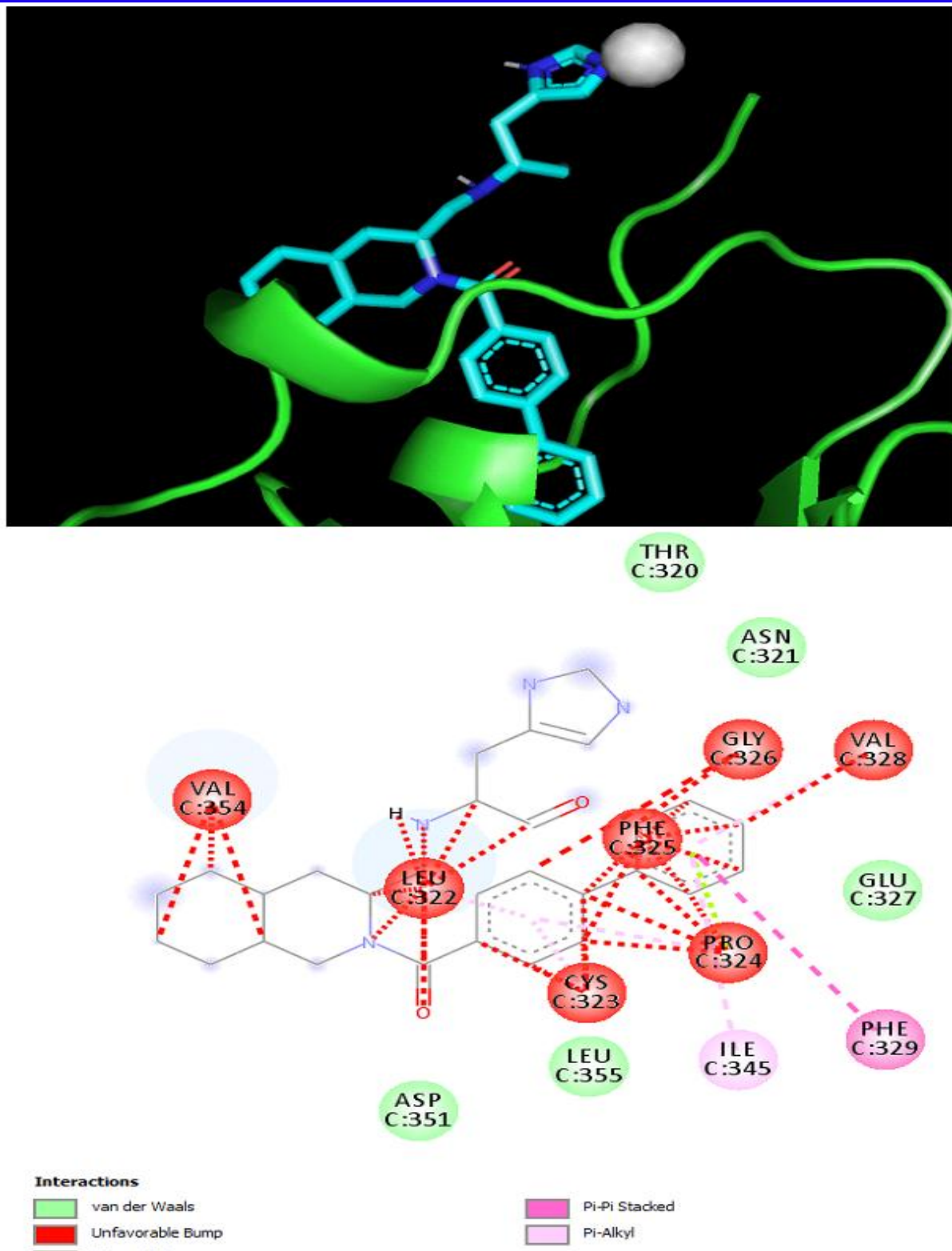
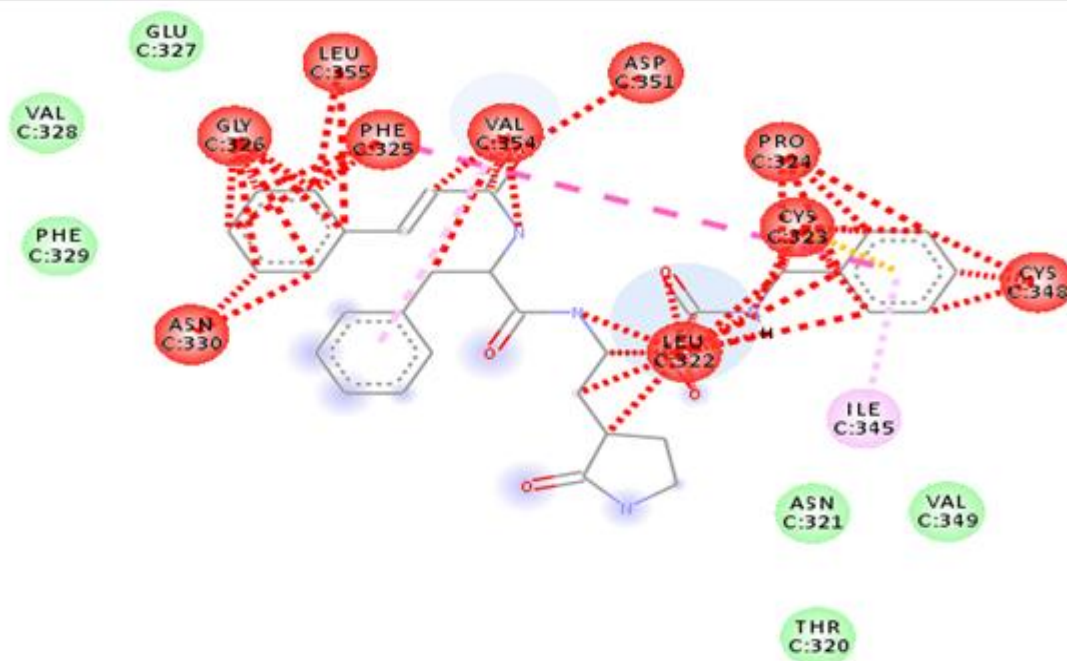
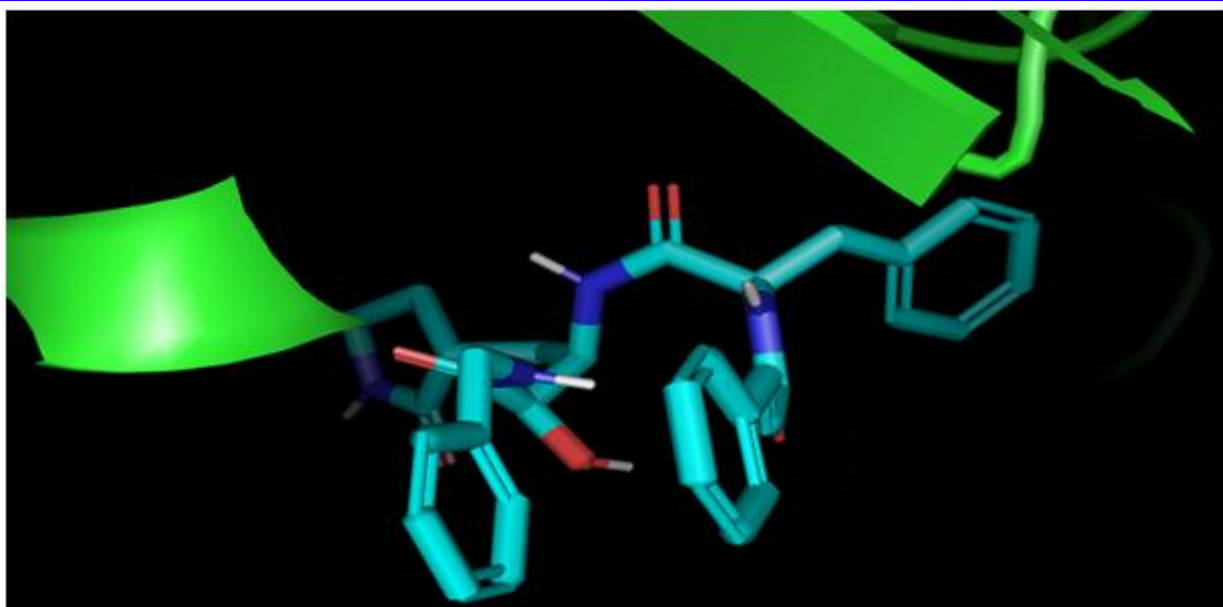


Figure 7a: Interactions of 4twy 3BL


Interactions

- █ van der Waals
- █ Unfavorable Bump
- █ Unfavorable Acceptor-Acceptor

- █ Pi-Sulfur
- █ Pi-Pi Stacked
- █ Pi-Alkyl

Figure 7b: Interactions of 5n19 D03

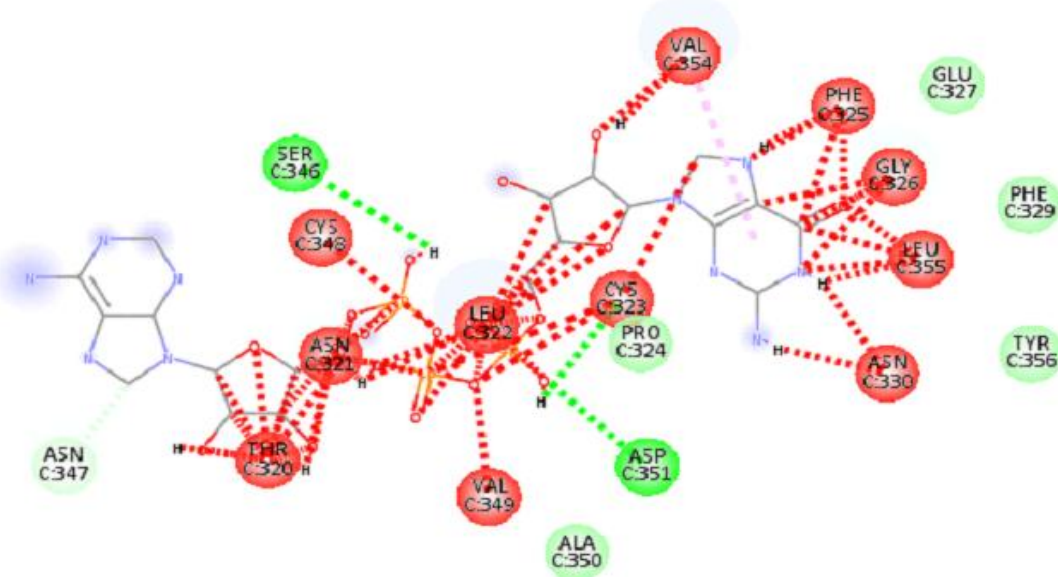
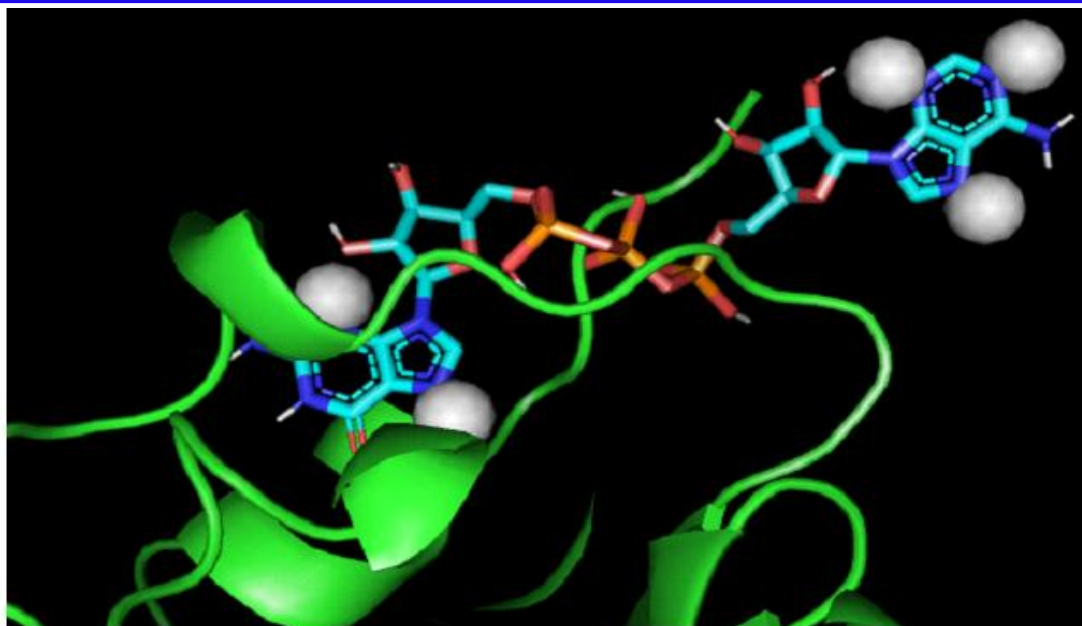
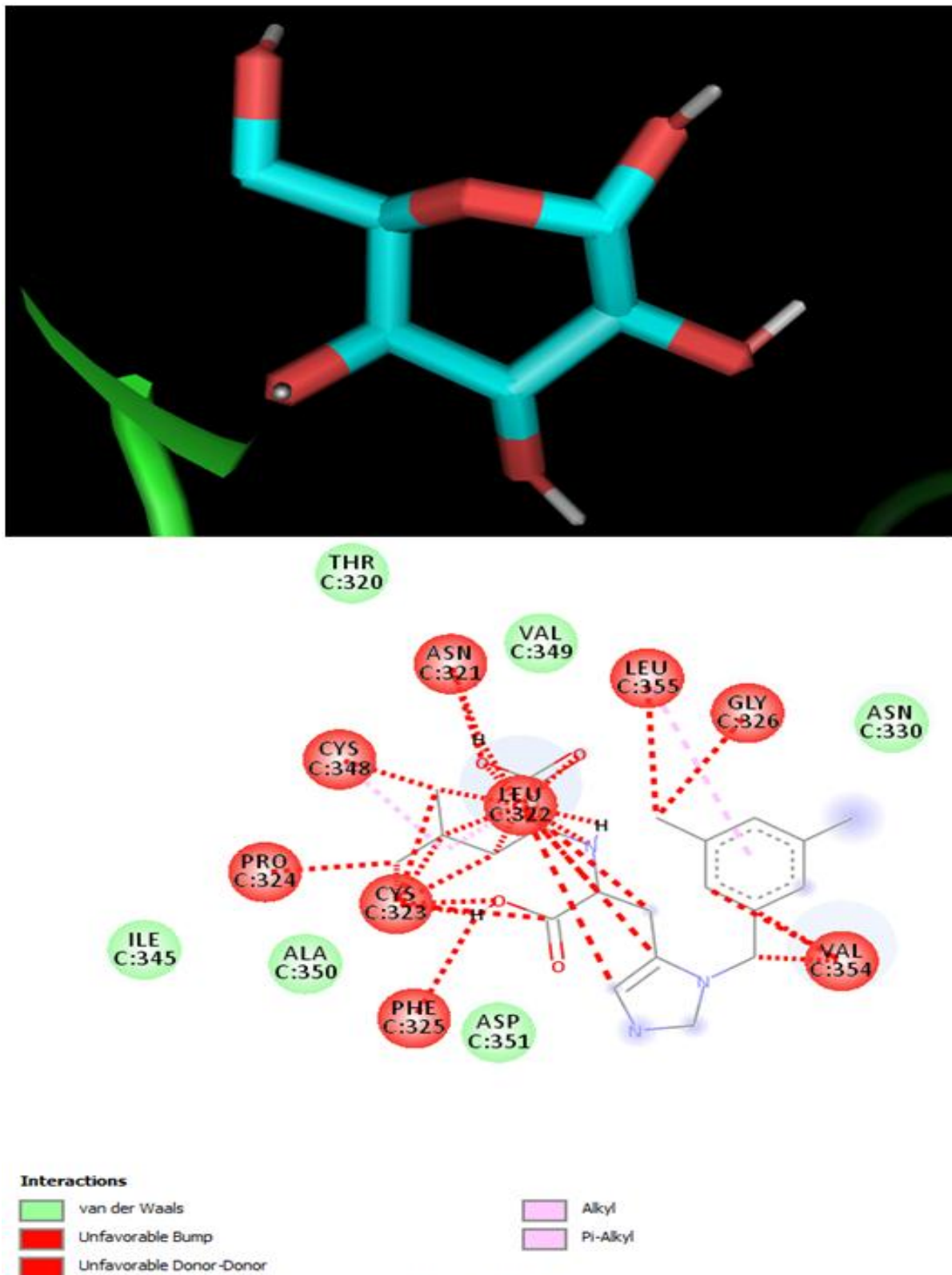


Figure 7c: Interactions of 5c8s G3A



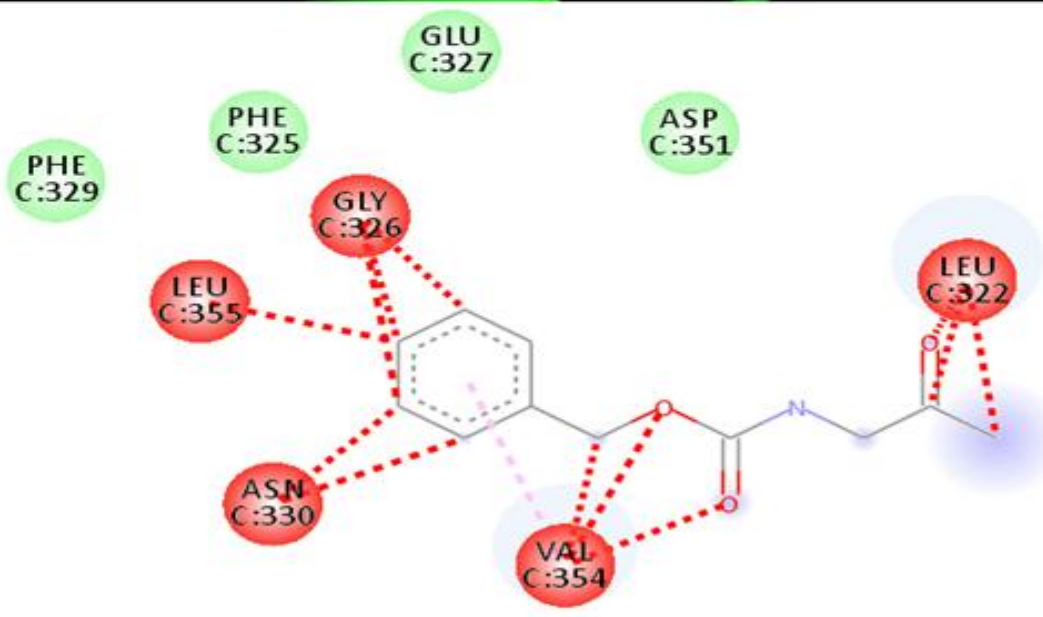
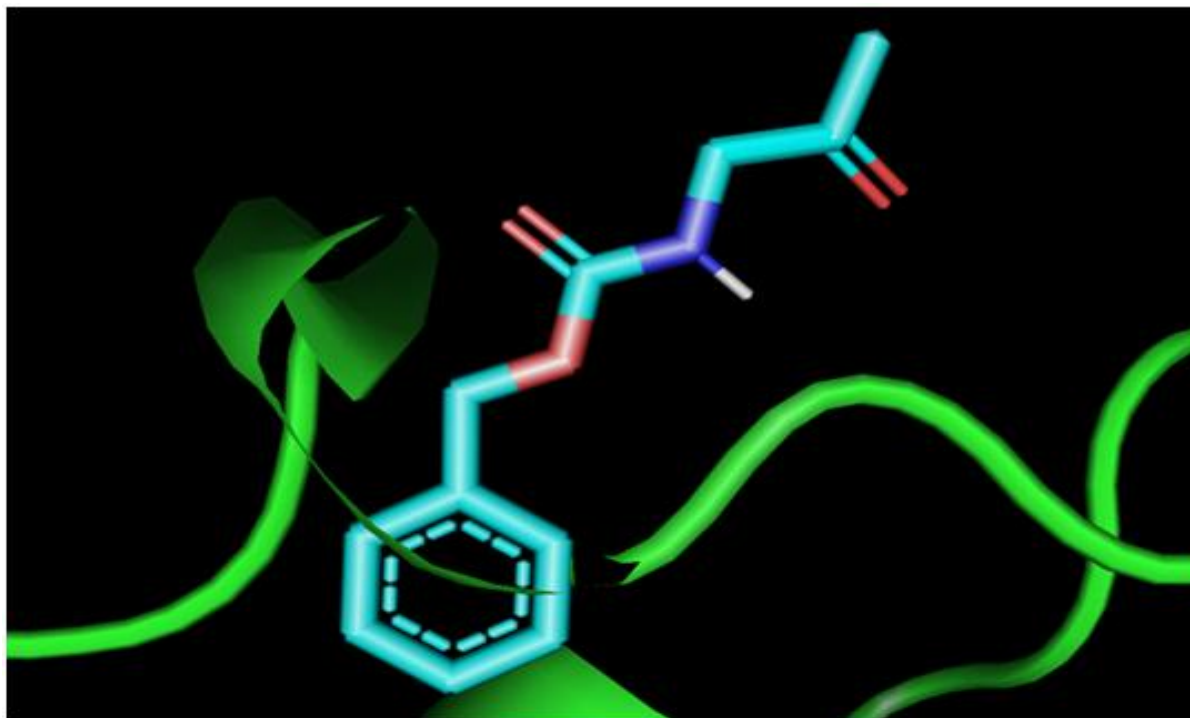
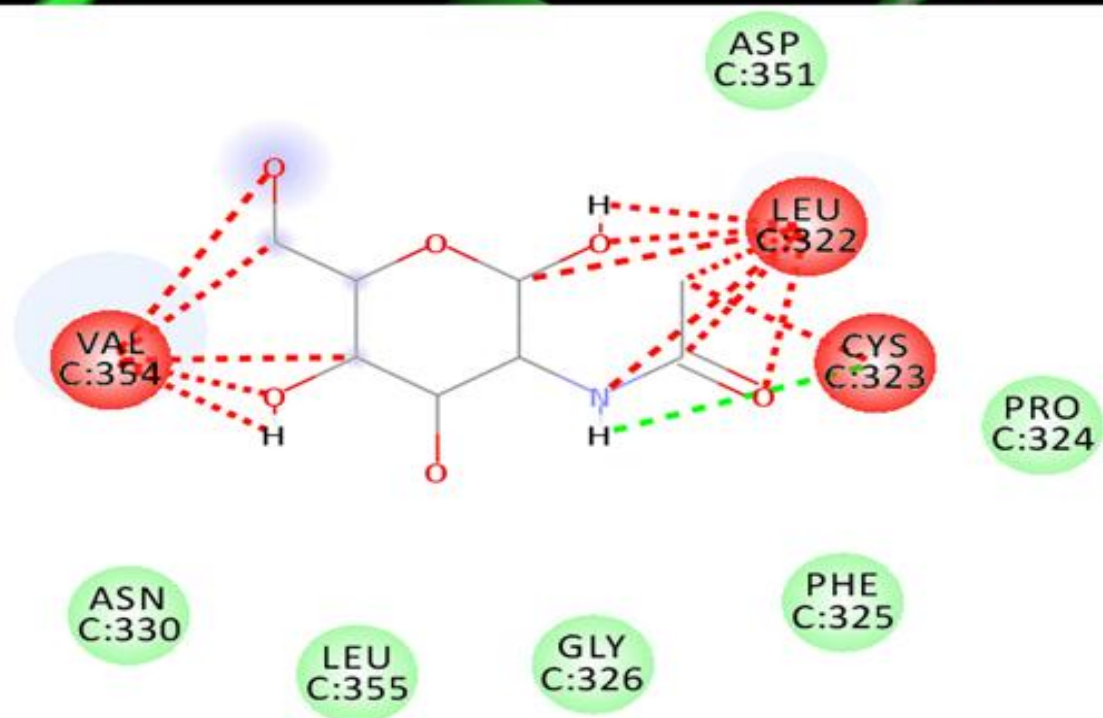
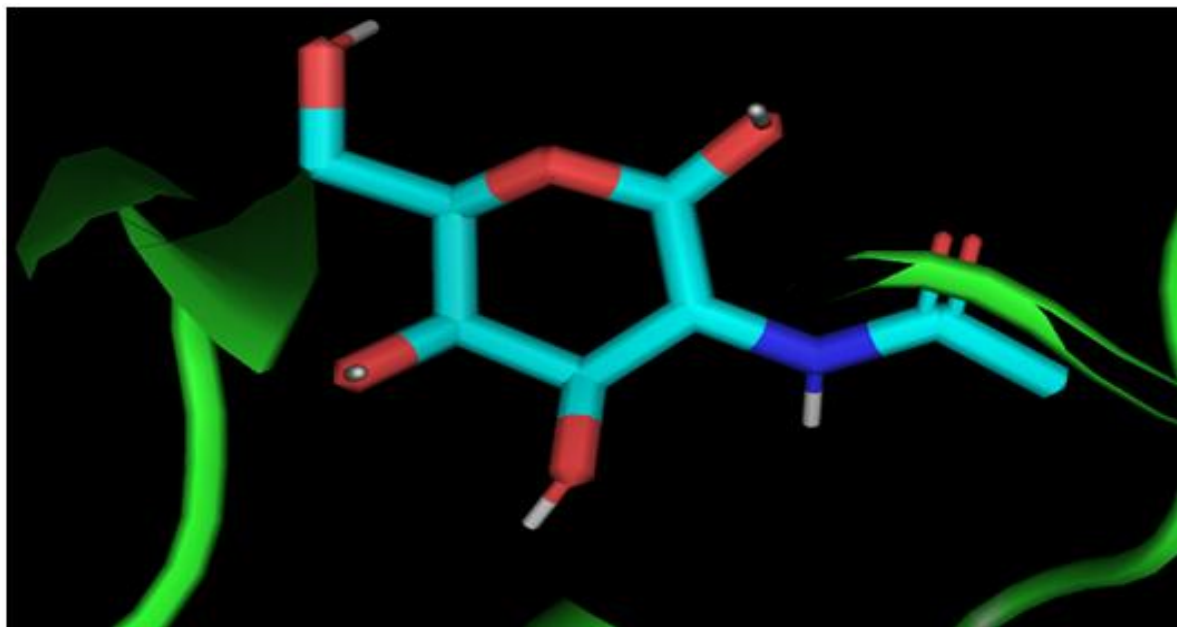


Figure 7e: Interactions of 3d62 959



Interactions

-  van der Waals
-  Unfavorable Bump

-  Conventional Hydrogen Bond

Figure 7f: Interactions of 1r4l NAG

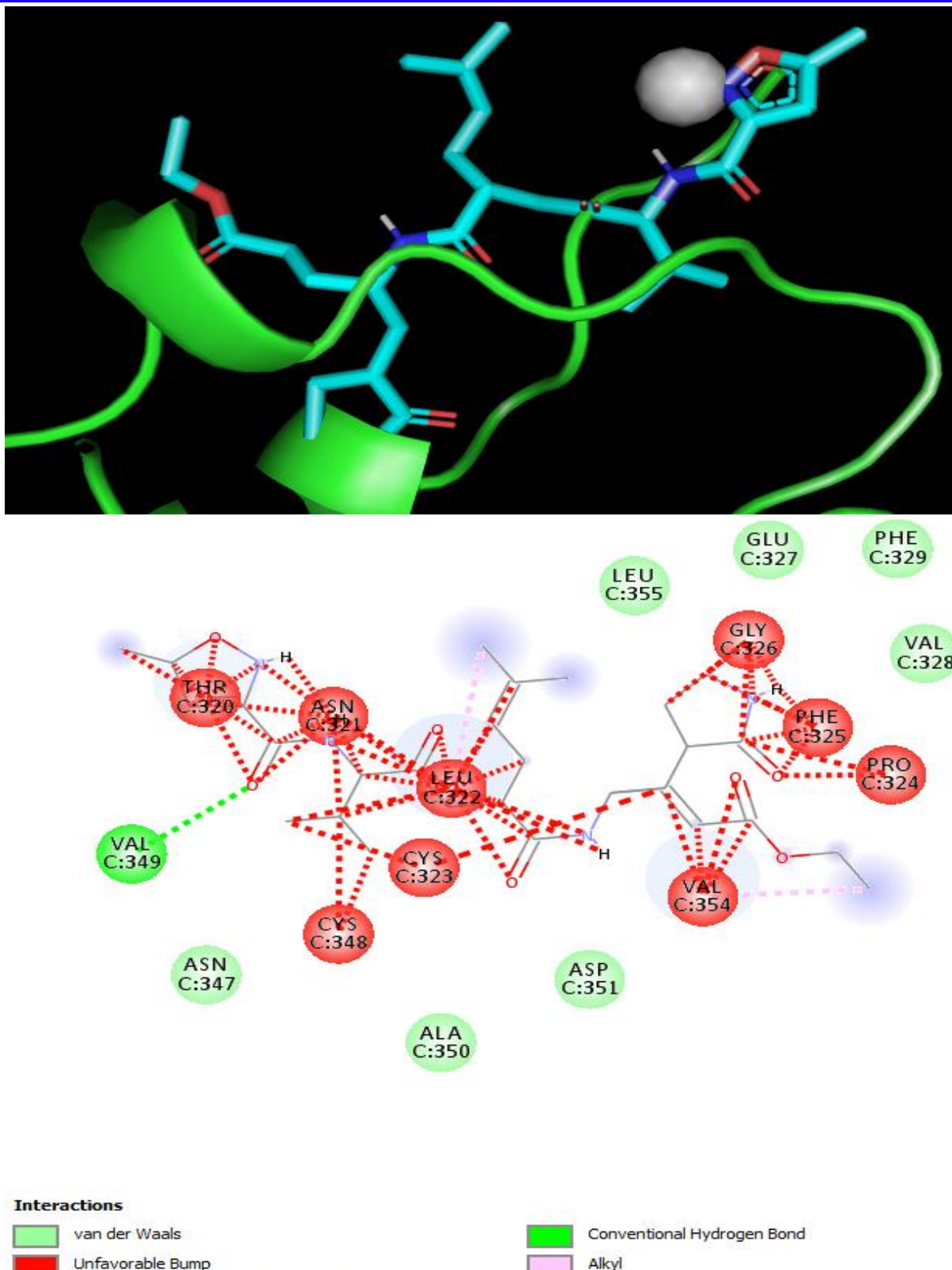


Table 3: Interacting residues in spike protein active site.

| S/N | Compound | Binding affinity (Kcal/mol) | Unfavorable Interactions | Favorable Interactions |
|-----|----------|-----------------------------|---|---|
| 1 | 4twy 3BL | -7.3 | GLY C:326, VAL C: 328, VAL C:354, LEU C:322, PHE C:325, CYS C:323, PRO C:324 | THR C:320, ASN C:321, GLU C:327, LEU C:355, ASP C:351, ILE C345, PHE C:329 |
| 2 | 5n19 D03 | -7.3 | LEU C:355, GLY C:326, ASN C:330, PHE C:325, VAL C:354, ASP C:351, PRO C:324, CYS C:323, CYS C:348, LEU C:322 | GLU C:327, VAL C:328, PHE C:329, ASN C:321, VAL C:349, THR C:320, ILE C:345 |
| 3 | 5c8s G3A | -6.8 | VAL C:354, PHE C:325, GLY C:326, LEU C:355, ASN C:330, CYC C:323, LEU C:322, VAL C:349, CYS C:348, ASN C:321, THR C:320 | SER C:346, ASP C:351, PRO C:324, ALA C:350, ASN C:347, GLU C:327, PHE C:329, TYR C:356 |
| 4 | 2alv CY6 | -6.8 | THR C:320, ASN C:321, LEU C:322, CYS C:323, CYS C:348, VAL C:354, GLY C:326, PHE C:325, PRO C:324 | VAL C:349, ASN C:347, ALA C:350, ASP C:351, LEU C:355, GLU C:327, PHE C:329, VAL C:328 |
| 5 | 2d2d ENB | -6.4 | PHE C:325, GLY C:326, PRO C:324, CYS C:323, LEU C:322, VAL C:354, ASN C:321, CYS C:348, ASN C:347, SER C:346 | ASP C:351, ASN C:330, LEU C:355, ILE C:345, VAL C:328, PHE C:329, GLU C:327, VAL C:349, THR C:320 |
| 6 | 2gx4 NOL | -6.3 | PHE C:325, LEU C:322, GLY C:326, PRO C:324, LEU C:322, CYC C:323, CYS C:348, SER C:346 | PHE C:329, GLU C:327, ASN C:330, ALA C:350, ILE C:345, ASP C:351, VAL C:354, ASN C:321, VAL C:349, THR C:320, ASN C:347 |
| 7 | 1wof I12 | -6.3 | THR C:320, ASN C:321, LEU C:322, CYS C:323, PRO C:324, PHE C:325, GLY C:326, SER C:346, ASN C:347, CYS C:348, VAL C:354, LEU C:355, VAL C:349 | GLU C:327, VAL C:328, PHE C:329, ASN C:330, ASP C:351, ASN C:381, SER C:380, ILE C:345, ALA C:350 |
| 8 | 3r24 SAM | -6.3 | ASN C:321, LEU C:322, VAL C:354, GLY C:326, LEU C:355, ASN C:330 | THR C:320, CYS C:348, VAL C:349, CYS C:323, PRO C:324, PHE C:325, GLU C:327, PHE C:329, TYR C:356 |

| | | | | |
|----|-----------|------|---|--|
| 9 | 3d62 959 | -5.9 | LEU C:322, GLY C:326, ASN C:330, VAL C:354, LEU C:355 | PHE C:325, GLU C:327, PHE C:329, ASP C:351 |
| 10 | 1r4l XX5 | -5.4 | VAL C:354, GLY C:326, LEU C:355, ASN C:321, LEU C:322, CYS C:348, PRO C:324, PHE C:325, CYS C:323 | THR C:320, VAL C:349, ASN C:330, ILE C:345, ALA C:350, ASP C:351 |
| 11 | *1r4l NAG | -4.8 | VAL C:354, LEU C:322, CYS C:323 | ASP C:351, PRO C:324, PHE C:325, GLY C:326, LEU C:355, ASN C:330 |

* *Cellular (native) ACE2*

A ligand may possess high binding affinity with a receptor but having many unfavorable interactions may negate the *in vivo* and *in vitro* activities of the ligand.

Highly Competitive Interactions can Serve Useful Biochemical Purposes

Availability of good chances of favourable interaction in a reacting system determines the feasibility of a reaction to yield more stable product [55]. For instance, from figures 7a to 7g and table 3, 1r4l NAG (cellular ACE2) in the domain of unfavourable interaction is competing with 4twy 3BL, 5n19 D03, 5c8s G3A, 2alv CY6, 2d2d ENB, and 1r4l XX5 for VAL C:354, LEU C:322 and CYS C:323 residues. While in the domain of favourable interaction, it is competing with 4twy 3BL for ASP C:351 and LEU C:355 residues. 4twy 3BL is having a residue for residue match of 50% with 1r4l NAG while the highest match of 60% as seen in the competition between receptor and 5c8s G3A and 2d2d ENB (table 4b), where ACE2 (1r4l NAG) was seen competing with the ligands for VAL C:354, LEU C:322, CYS C:323, ASP C:351, PRO C:324 and CYS C:323 in the case of 5c8s G3A; and VAL C:354, LEU C:322, CYS C:323, ASN C:330, ASP C:351 and LEU C:355 residues in the case of 2d2d ENB (table 4b). With higher binding affinity and having more interacting residues in common with the native ligand, it is expected that these exogenous ligands displace the native ligand from the receptor binding pocket to produce an observable physicochemical change that can translate into pharmacologic response and serve as diagnostic biomarker for the particular receptor.

1r4l NAG made favourable interactions where 4twy 3BL made unfavourable contacts with PRO C:324, GLY C:326, PHE C:325 and CYS C:323. 5n19 D03 made unfavourable interactions with ASN C:330, ASP C:351, PRO C:324, LEU C:355, GLY C:326, PHE C:325 and CYS C:323. 5c8s G3A made unfavourable interactions with ASN C:330, LEU C:355, GLY C:326, PHE C:325 and CYS C:323. CYS C:323 also had a conventional hydrogen bond in 1r4l NAG. Apart from CYS C:323, 5c8s G3A also possesses two more hydrogen bonds at SER C:346 and ASP C: 351 residues. 5c8s G3A in addition captured many other residues not found in 1r4l NAG such as: ASN C:347, THR C:320, ASN C:321, CYS C:348, VAL C:349, ALA C:350, TYR C:356, PHE C:329, GLU C:327 and importantly, ASP C:351 and SER C:346 which were involved in hydrogen bond formation. ASP C:351 was also involved in hydrogen bond formation with 2d2d ENB. 2d2d ENB is seen making unfavourable interaction with PRO C:324, GLY C:326, PHE C:325 and CYS C:323. 2alv G3A made its unfavourable interactions at receptor residues PRO C:324, GLY C:326, PHE C:325 and CYS C:323. From the observations here, 5c8s G3A and 2d2d ENB constitute

agents to achieve useful pharmacologic and diagnostic purposes on SARS-CoV-2 research endeavour.

Availability of more favourable interactions than unfavourable interactions suggest that the product formed will be more stable (table 4a and figure 8). Of the ligands that interacted with the spike protein, ACE2 (1r4l NAG) had the highest percentage of favourable interactions but had fewer contacts with the receptor residues than the trailing exogenous ligands.

Table 4a: Quantization of favourable and unfavourable interactions among ligands.

| Ligand | Unfavourable Interaction (UI) | Favourable Interaction (FI) | Total | % FI |
|----------|-------------------------------|-----------------------------|-------|------|
| 1r4l NAG | 3 | 6 | 9 | 66.7 |
| 3r24 SAM | 6 | 9 | 15 | 60 |
| 2gx4 NOL | 8 | 11 | 19 | 57.9 |
| 4twy 3BL | 7 | 7 | 14 | 50 |
| 2d2d ENB | 10 | 9 | 19 | 47.4 |
| 2alv CY6 | 9 | 8 | 17 | 47.1 |
| 3d62 959 | 5 | 4 | 9 | 44.4 |
| 5c8s G3A | 11 | 8 | 19 | 42.1 |
| 5n19 D03 | 10 | 7 | 17 | 41.2 |
| 1wof I12 | 13 | 9 | 22 | 40.9 |
| 1r4l XX5 | 9 | 6 | 15 | 40 |

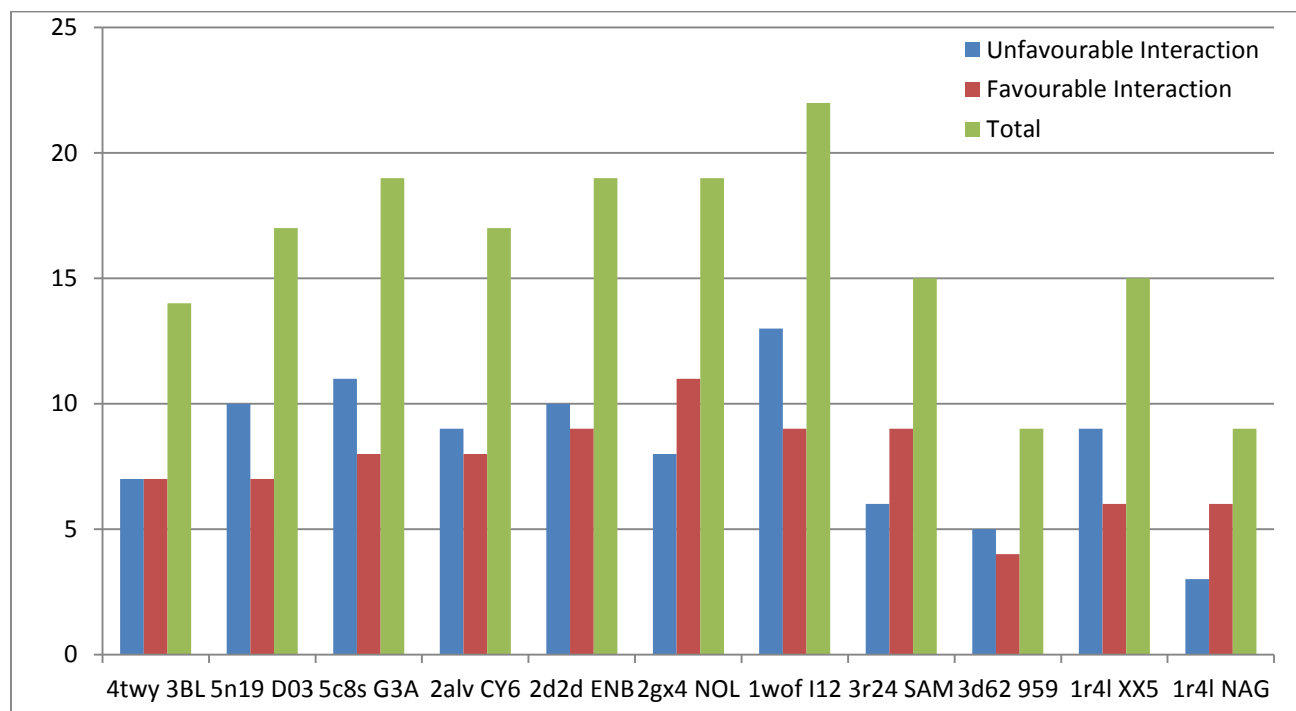


Figure 8: Distribution of favourable and unfavourable interactions between ligands and sars-cov-2 spike protein receptor residues.

Table 4b: Percentage residue matching between exogenous ligands and ace2 on the spike protein binding pocket

| Ligand | Unfavourable Interaction | | | | Favourable Interaction | | | | | H-Bond | % Match | |
|----------|--------------------------|-----------|-----------|-----------|------------------------|-----------|-----------|-----------|-----------|-----------|---------|----|
| | *1r4l NAG | VAL C:354 | LEU C:322 | CYS C:323 | ASN C:330 | ASP C:351 | PRO C:324 | LEU C:355 | GLY C:326 | PHE C:325 | | |
| 4twy 3BL | YES | YES | YES | YES | NO | YES | NO | YES | NO | NO | NO | 50 |
| 5n19 D03 | YES | YES | YES | YES | NO | NO | NO | NO | NO | NO | NO | 30 |
| 5c8s G3A | YES | YES | YES | NO | YES | YES | NO | NO | NO | YES | YES | 60 |
| 2alv CY6 | YES | YES | YES | NO | YES | NO | YES | NO | NO | NO | NO | 50 |
| 2d2d ENB | YES | YES | YES | YES | YES | NO | YES | NO | NO | NO | NO | 60 |
| 2gx4 NOL | NO | YES | YES | YES | YES | NO | NO | NO | NO | NO | NO | 40 |
| 1wof I12 | YES | YES | YES | YES | YES | NO | NO | NO | NO | NO | NO | 50 |
| 3r24 SAM | YES | YES | NO | NO | NO | YES | NO | NO | NO | YES | NO | 40 |
| 3d62 959 | YES | YES | NO | NO | YES | NO | NO | NO | NO | YES | NO | 40 |
| 1r4l XX5 | YES | YES | YES | YES | YES | NO | NO | NO | NO | NO | NO | 50 |

* Endogenous ACE2 binding SARS-CoV-2 spike protein in the cell.

“Yes” stands for a position on the binding pocket where ACE2 and ligand share same interacting residue, “No” stands for a position on the binding pocket where ACE2 and ligand are not sharing same interacting residue.

Evaluation of druglikeness and organ toxicity of some selected hits

The lipophilicity for selected compounds is as shown by the values of their consensus LogP in table 5.

Table 5: Comparison of cLogP and miLogP values for the selected compounds as seen in SwissADMET and Molinspiration platforms respectively

| S/N | Molecule | SwissADMET cLogP | Molinspiration LogP | Mean LogP |
|-----|----------|------------------|---------------------|-----------|
| 1 | 4TWY 3BL | 3.97 | 4.60 | 4.29 |
| 2 | 5N19 D03 | 2.66 | 2.39 | 2.53 |
| 3 | 5C8S G3A | -5.47 | -4.67 | -5.10 |
| 4 | 2ALV CY6 | 3.07 | 2.67 | 2.87 |
| 5 | 2D2D ENB | 2.57 | 4.46 | 3.52 |
| 6 | 2GX4 NOL | 3.14 | 5.04 | 4.10 |
| 7 | 1WOF I12 | 1.94 | 1.10 | 1.52 |
| 8 | 3R24 SAM | -2.96 | -4.14 | -3.55 |
| 9 | 3D62 959 | 1.46 | 1.09 | 1.28 |
| 10 | 1R4L XX5 | 2.06 | 0.28 | 1.17 |

cLogP = octanol/water coefficient.

Druglikeness of the compounds are shown in tables 6a and b

Table 6a: Druglikeness of selected compounds based on Lipinski, Veber and Ghose rule

| S/N | Molecule | Mw(g/mol) | TPSA (Å ²) | No of HBA | No of HBD | No of RB | cLogP |
|-----|----------|-----------|---------------------------|--------------|--------------|-------------|-------|
| 1 | 4TWY 3BL | 470.61 | 78.09 | 4 | 2 | 9 | 3.97 |
| 2 | 5N19 D03 | 568.66 | 136.63 | 5 | 5 | 16 | 2.66 |
| 3 | 5C8S G3A | 772.41 | 436.84 | 22 | 10 | 12 | -5.47 |
| 4 | 2ALV CY6 | 558.67 | 156.70 | 8 | 3 | 18 | 3.07 |
| 5 | 2D2D ENB | 558.67 | 151.93 | 7 | 4 | 18 | 2.57 |
| 6 | 2GX4 NOL | 602.76 | 155.09 | 7 | 5 | 19 | 3.14 |
| 7 | 1WOF I12 | 618.72 | 197.83 | 9 | 5 | 21 | 1.94 |
| 8 | 3R24 SAM | 398.44 | 210.76 | 9 | 4 | 7 | -2.96 |
| 9 | 3D62 959 | 207.23 | 55.40 | 3 | 1 | 6 | 1.46 |
| 10 | 1R4L XX5 | 428.31 | 104.45 | 6 | 3 | 10 | 2.06 |

Table 6b: Druglikeness of selected molecules based on Lipinski, Veber and Ghose rule continued

| S/N | Molecule | Lipinski Filter | Veber Filter | Ghose Filter |
|-----|----------|---|---------------------------------------|---|
| 1 | 4TWY 3BL | Yes; 0 violation | Yes | No; 1 violation: MR>130 |
| 2 | 5N19 D03 | Yes; 1 violation: MW>500 | No; 1 violation: Rotors>10 | No; 3 violations: MW>480, MR>130, #atoms>70 |
| 3 | 5C8S G3A | No; 3 violations: Mw>500, NorO>10, NHorOH>5 | No; 2 violations: Rotors>10, TPSA>140 | No; 4 violations: MW>480, WLOGP<-0.4, MR>130, #atoms>70 |
| 4 | 2ALV CY6 | No; 2 violations: MW>500, NorO>10 | No; 2 violations: Rotors>10, TPSA>140 | No; 3 violations: MW>480, MR>130, #atoms>70 |
| 5 | 2D2D ENB | No; 2 violations: MW>500, NorO>10 | No; 2 violations: Rotors>10, TPSA>140 | No; 3 violations: MW>480, MR>130, #atoms>70 |

| | | | | |
|----|----------|---|--|--|
| 6 | 2GX4 NOL | No; 2 violations: MW>500, NorO>10 | No; 2 violations: Rotors>10, TPSA>140 | No; 3 violations: MW>480, MR>130, #atoms>70 |
| 7 | 1WOF I12 | No; 2 violations: MW>500, NorO>10 | No; 2 violations: Rotors>10, TPSA>140 | No; 3 violations: MW>480, MR>130, #atoms>70 |
| 8 | 3R24 SAM | Yes; 1 violation: NorO>10 | No; 1 violation: TPSA>140 | No; 1 violation: WLOGP<-0.4 |
| 9 | 3D62 959 | Yes; 0 violation | Yes | Yes |
| 10 | 1R4L XX5 | Yes; 0 violation | Yes | Yes |

Cramer rules for Toxicological Hazard Estimation from Molecular Structure (when administered orally) by Decision Tree Approach using Toxtree v2.6.13 indicated that none of the selected ligands is a normal constituent of the body and they do not contain functional groups associated with enhanced toxicity. This position was maintained when visualized by applying Carcinogenicity (genotox and nongenotox) and mutagenicity rule base by ISS Predicts to predict the possibility of carcinogenicity and mutagenicity by discriminant analysis and structural rules in the same platform.

DISCUSSIONS

The presence of conventional hydrogen bond in cellular ACE 2 (1r4l NAG) can confer adequate resistance against displacement by any ligand of high binding affinity without a hydrogen bond suitably in the same position of amino acid residue as seen in ACE2. The presence of a conventional hydrogen bond therefore can pose a resistance in attempt to displace viral spike protein from cell surface except in situations where exogenous ligands adequately matched it with enough suitable bonds as we have in 5c8s G3A and 2d2d ENB.

The amino acids that dominated interaction between spike and ACE2 in the binding pocket constitute the most important targets in any interaction aimed at interfering with binding of ACE2 to spike protein. Considering the ten selected ligands, ligands with amino acids matching most of those involved in interaction between ACE2, and possessing high binding affinity will be favourably disposed to elicit maximum activity against the viral spike protein. 1r4l NAG (ACE2) exhibited much lower binding affinity to spike protein than many of the spike protein ligands. This implies that spike protein can be inhibited from binding to ACE2 or ACE2 can easily be displaced from binding pocket in the presence of any of the molecules which have higher binding affinity thereby disrupting cell invasion by the virus. The highest binding affinity attained by ACE2 is -4.8Kcal/mol whereas a spike protein ligand 4twy 3BL has -7.3Kcal/mol.

Efficient complex formation between ligands and receptors can also be utilized as diagnostic makers when they yield distinctive characteristic reactions such as precipitation, colour change,

gas production or change in temperature following the interaction between the ligand and receptors [56], [57]. A detection method could also be electrochemical or fluorescence [58], aimed at detecting the presence of target molecules in biological samples that are known to bind to the receptor [59] and the amount of precipitate, colour, gas or temperature change determines the level of the viral protein present, implying that the assay can be qualitative and quantitative.

In vivo activities of replicase protein 1uw7 (nsp9) from this study is likely to be disrupted by quite a good number of ligands as many ligands demonstrated high binding affinity with the receptor. Of the many ligands that exhibited high binding affinity with the two receptors, only those whose binding affinities in the first orientation ranged from -7.3 to -4.8 and -8.2 to -5.0 Kcal/mol for 2ghv and 1uw7 respectively were selected for analysis. The complexes formed by some of the ligands are represented in figures 5 and 6. From the figures, it could be observed that autodock structures appear to have different modification from their sdf counterparts seen in figures 2 and 3. Target analysis of some of the selected ligands was done only for ligands which showed high level of binding affinity, including ACE2 to the receptors. Visualization of binding pockets, nature and strength of interaction between ligands and receptor residues were the parameters considered.

Among the selected ligands, only 3d62 959 and 1r4l XX5 exhibited complete druglike properties based on Lipinski, Veber and Ghose rules. 3d62 959 has 40% and 1r4l XX5 has 50% of its residue matching those of ACE2 in the receptor binding pocket, with no hydrogen bonds. 3d62 959 also has many of its residues forming unfavourable bonds and CYS C:323, ASN C:330 and PRO C:324 not forming any bond at all. All these indicate lower competitiveness among the rest of the ligands against ACE2 for spike protein receptor.

SUMMARY OF FINDINGS

In this study, an extensive study was carried out in silico to discover molecules that could be of medical use for management of COVID-19 in the areas of diagnosis and treatment. Ligands (or small molecules or drugs) with activity against SARS-CoV-2 spike and replicase proteins were extracted from designated drugs and proteins databases. The ligands were screened against the receptors (SARS-CoV-2 spike and replicase proteins) to isolate molecules that can favourably bind these receptors thus displacing or inhibiting binding of their endogenous or native ligands – acetylcholinesterase 2 (ACE2) in the case of spike protein to inhibit viral attachment to the host cells.

Ninety ligands were screened out of which 10 were found to have higher binding affinity with spike protein (PDB ID: 2ghv) than ACE2 (PDB ID: 1r4l NAG), with binding affinity ranging from -7.3 to -4.8 (table 2a). These higher binding affinity ligands were isolated for further in silico evaluations. Their analysis showed 5c8s G3A and 2d2d ENB as the most suitable leads that are favourably disposed for SARS-CoV-2 spike protein detection from biological samples, while 3d62 959 and 1r4l XX5 were identified as leads with most suitable druglikeness against SARS-CoV-2 based on the filters from SwissADME and Molinspiration cheminformatics and therefore deserve further in vitro and in vivo evaluations. Notwithstanding, due to their disposition to favourable interaction with the receptor residues, 5c8s G3A and 2d2d ENB can also be applied in SARS-CoV-2 treatment following adequate in vitro and in vivo safety considerations.

In silico drugability testing of the 10 selected compounds indicates that only two compounds (3d62 959 and 1r4l XX5) suitably satisfied all safety conditions of druglikeness based on Lipinsky, Veber

and Ghose rules (tables 6a and 6b), implying that they can be administered to mimic the native form of the ligand in binding viral spike protein.

CONCLUSION

Following the analysis and observations so far, all the 10 selected compounds having higher binding affinity with viral spike protein than ACE2 deserve further in vitro and in vivo evaluations to determine which compound has the best in vivo activity against SARS-CoV-2 spike and replicase proteins, and safe for human use and also efficient in detecting viral proteins from biological samples with high precision.

RECOMMENDATIONS

This study therefore recommends repurposing the use of 5c8s G3A, 2d2d ENB, 3d62 959 and 1r4l XX5 in further studies of COVID-19 treatment and possible alternative diagnostic approach.

Limitation of the Study

Replicase protein was not able to yield into any molecular visualization software therefore its interaction patterns were not analyzed.

Funding Sources

The author received no financial support for the research, authorship, and publication of this article.

Conflict of Interest

The authors declares no conflict of interest.

REFERENCES

1. Alexandra C. Walls, Young-Jun Park, Alejandra M. Tortorici, Abigail Wall, Andrew T. McGuire and David Veesler, (2020). Structure, Function, and Antigenicity of the SARS-CoV-2 Spike Glycoprotein. Volume 181, issue 2, 16 April 2020, Page 281-292.ed doi 10.1016/j.cell.2020.02.058. Epub 2020 Mar 9.
2. Chen Y.W., Yiu C. P. B and Wong K. Y., (2020). Prediction of the SARS-CoV-2 (2019-nCoV) 3C-like protease (3CLpro) structure: virtual screening reveals velpatasvir, ledipasvir, and other drug repurposing candidates, *F1000 Research*, vol. 9, p. 129, 2020.
3. Wang C., Phorby P. W, Hayden F. G, and Gao G. F., (2020). “A novel coronavirus outbreak of global health concern,” *Ge Lancet*, vol. 395, no. 10223, pp. 470–473, 2020.
4. World Health Organization Advancing the right to health: the vital role of law Limiting contact with infectious persons. <https://www.who.int/healthsystems/topics/health-law/chapter10.pdf>.
5. European Centre for Disease Prevention and Control, (2020). Case Definition for Coronavirus Disease 2019 (COVID-19), as of 3 December 2020.

6. Andres F. Yepes-Pérez, Oscar Herrera-Calderon, Jose'-Emilio Sa'nchez-Aparicio, Laura Tiessler-Sala, Jean-Didier Mare'chal, and Wilson Cardona-G, (2020). Investigating Potential Inhibitory Effect of *Uncaria tomentosa* (Cat's Claw) against the Main Protease 3CLproof SARS-CoV-2 by Molecular Modeling. Evidence-Based Complementary and Alternative Medicine Volume 2020, Article ID 4932572, 14 pages
<https://doi.org/10.1155/2020/4932572>.
7. Institute of Medicine (US) Forum on Microbial Threats. Global Infectious Disease Surveillance and Detection: Assessing the Challenges—Finding Solutions, Workshop Summary. Washington (DC): National Academies Press (US), 2007. Summary and Assessment. Available from: <https://www.ncbi.nlm.nih.gov/books/NBK52862/>.
8. Li H., (2011). Ligand Binding Can Influence the Mechanical Stability of Proteins. H. Li, in Comprehensive Nanoscience and Technology.
9. Michael Blaber, (2001). BCH 4053 Biochemistry I. Enzyme Inhibition, Reactions Involving Two or More Substrates, Ribozymes and Abzymes. *Lecture 25*, Fall 2001.], [[Avick Kumar Ghosh](#), [Indranil Samanta](#), [Anushree Mondal](#), [Prof. Dr. Wenshe Ray Liu](#)(2019). Covalent Inhibition in Drug Discovery. First published: 27 February 2019
<https://doi.org/10.1002/cmdc.201900107>.
10. [Ekins S.](#), [Mestres J](#), and [Testa B.](#), (2007). *In silico* pharmacology for drug discovery: applications to targets and beyond Sep; 152(1): 21–37. [Br J Pharmacol](#). Published online 2007 Jun 4. doi: [10.1038/sj.bjp.0707306](https://doi.org/10.1038/sj.bjp.0707306) PMID: [PMC1978280](#) PMID: [17549046](#).
11. Janet Piñero, Laura I. Furlong, Ferran Sanz, (2018). *In silicomodels* in drug development: where we are. Article in Current Opinion in Pharmacology · September 2018 DOI:10.1016/j.coph.2018.08.007.
12. Francis E. Agamah, Gaston K. Mazandu, Radia Hassan, Christian D. Bope, Nicholas E. Thomford, Anita Ghansah and Emile R. Chimusa, (2019). Computational/in silico methods in drug target and lead prediction. Corresponding author: Emile R. Chimusa, University of Cape Town, Division of Human Genetics, Department of Pathology, University of Cape Town, Observatory 7925, South Africa. E-mail: emile.chimusa@uct.ac.za.
13. [Qifeng Bai](#), Lanlan Li, Shanhui Liu, Shujun Xiao and Yu Guo, (2018). Drug Design Progress of In silico, In vitro and In vivo Researches.
14. Prajapat, M., Sarma, P., Shekhar, N., Avti, P., Sinha, S., Kaur, H., Kumar, S., Bhattacharyya, A., Kumar, H., Bansal, S., and Medhi, B., (2020). Drug targets for corona virus: A systematic review. Indian Journal of Pharmacology, 52(1), 56.
https://doi.org/10.4103/ijp.IJP_115_20.
15. WHO Q&A on COVID-19, 15 April, 2020, retrieved on October 31, 2020.
16. Zhu H, Rhee J W, Cheng P, Amy CH, Mark M D, et al., (2020). Cardiovascular Complications in Patients with COVID-19: Consequences of viral Toxicities and Host Immune Response. Curr CardiolRep 22(5): 32-36.

17. Helms J, Kremer S, Merdji H, Cere R, Malika S, et al., (2020). Neurologic Features in Severe SARS-cOv-2 Infection. *N Engl J Med* 382:2268-2270.
18. John Hopkins University (JHU) Through World Health Organization, The European Centers for Disease Prevention and Control, and local health organizations.
19. Zhu H, Rhee J W, Cheng P, Amy CH, Mark M D, et al., (2020). Cardiovascular Complications in Patients with COVID-19: Consequences of viral Toxicities and Host Immune Response. *Curr CardiolRep* 22(5): 32-36.
20. Helms J, Kremer S, Merdji H, Cere R, Malika S, et al., (2020). Neurologic Features in Severe SARS-cOv-2 Infection. *N Engl J Med* 382:2268-2270.
21. Saldanha C., (2020). Erythrocte a Target for COVID-19 Infected Patients. *Mod ApproDrug Des.* 3(1).
22. Lamers M. M, Joep B, Jelte V, Kevin K, Jens, P, et al., (2020). SARS-CoV-2 Productively infect human gut enterocytes. *Science* 369 (6499): 50-54.
23. Cosic I, Cosic D and Lonarevic I., (2020). RRM Prediction of erythrocyte Band3 Protein as Alternative receptor for SARS-CoV-2 Virus. *Appl Sci* 10(11): 4053.
24. Jamwal S., Gautam A., Elsworth J., Kumar M., Chawla R., and Kumar P., (2020). An updated insight into the molecular pathogenesis, secondary complications and potential therapeutics of COVID-19 pandemic. *Life Sciences*, 257, 118105.
<https://doi.org/10.1016/j.lfs.2020.11810532687917>.
25. Wu J., Yuan X., Wang B., Gu R., Li W., Xiang X., Tang L., and Sun H., (2020). Severe Acute Respiratory Syndrome Coronavirus 2: From Gene Structure to Pathogenic Mechanisms and Potential Therapy. *Frontiers in Microbiology*, 11, 1576.
<https://doi.org/10.3389/fmicb.2020.01576> 32719672.
26. Jamwal S., Gautam A., Elsworth J., Kumar M., Chawla R., and Kumar P., (2020). An updated insight into the molecular pathogenesis, secondary complications and potential therapeutics of COVID-19 pandemic. *Life Sciences*, 257, 118105.
<https://doi.org/10.1016/j.lfs.2020.11810532687917>.
27. Muhammad Shehroz, Tahreem Zaheer and Tanveer Hussain, (2020). Computer-aided Drug Design Against Spike Glycoprotein of SARS-CoV-2 to Aid COVID-19 Treatment. *Han & Kral*, 2020. Volume 6, issue 10, October 2020, e05278.
28. William C Hwang, Yaqiong Lin, Eugenio Santelli, Jianhua Sui, Lukasz Jaroszewski Jaroszewski, Boguslaw Stec, Michael Farzan, Wayne A Marasco and Robert C. Liddington, (2006). Structural basis of neutralization by a human anti-severe acute respiratory syndrome spike protein antibody, 80R. *Affiliations PMID: 16954221 DOI: 10.1074/jbc.M603275200.*
29. Fehr A. R., Perlman S., (2015). Coronaviruses: An overview of their replication and pathogenesis. *Coronaviruses*: Springer; 2015. p. 1–23.

30. Glowacka I, Bertram S, Müller M. A, Allen P, Soilleux E, Pfefferle S, et al., (2011). Evidence that TMPRSS2 activates the severe acute respiratory syndrome coronavirus spike protein for membrane fusion and reduces viral control by the humoral immune response. *J Virol.* 2011;85(9):4122–34.
31. Qian Z, Dominguez S. R and Holmes K. V., (2013). Role of the Spike Glycoprotein of Human Middle East Respiratory Syndrome Coronavirus (MERS-CoV) in Virus Entry and Syncytia Formation. *PLoS One.* 2013;8(10):e76469.
32. Schoeman D., Fielding B. C., (2019). Coronavirus Envelope Protein: Current Knowledge. *Virol J* 16, 69 (2019). <https://doi.org/10.1186/s12985-019-1182-0>.
33. Venkatagopalan P, Daskalova S. M, Lopez L. A, Dolezal K. A and Hogue B. G., (2015). Coronavirus Envelope (E) Protein Remains at the Site of Assembly. *Virology.* 2015;478:75–85.
34. Nieto-Torres J. L, DeDiego M. L, Álvarez E, Jiménez-Guardeño J. M, Regla-Nava J. A, Llorente M, et al., (2011). Subcellular location and topology of severe acute respiratory syndrome coronavirus envelope protein. *Virology.* 2011;415(2):69–82.
35. Masters P. S., (2006). The Molecular Biology of Coronaviruses. *Adv Virus Res.* 2006;66:193–292.
36. Fehr A. R and Perlman S., (2015). Coronaviruses: An overview of their replication and pathogenesis. *Coronaviruses:* Springer; 2015. p. 1–23.
37. Escors D, Ortego J, Laude H and Enjuanes L., (2001). The membrane M protein carboxy terminus binds to transmissible gastroenteritis coronavirus core and contributes to core stability. *J Virol.* 2001;75(3):1312–24.
38. Narayanan K, Maeda A, Maeda J and Makino S., (2000). Characterization of the coronavirus M protein and nucleocapsid interaction in infected cells. *J Virol.* 2000;74(17):8127–34.
39. Snijder E. J, Decroly E, and Ziebuhr J., (2016). The Nonstructural Proteins Directing Coronavirus RNA Synthesis and Processing PMCID: PMC7112286 PMID: 27712628.
40. de Haan C. A and Rottier P. J., (2005). Molecular Interactions in the Assembly of Coronaviruses. *Adv Virus Res.* 2005; 64:165–230.
41. McBride R, van Zyl M and Fielding B. C., (2014). The coronavirus nucleocapsid is a multifunctional protein. *Viruses.* 2014; 6(8):2991–3018.
42. Geoff Sutton, Elizabeth Fry, Lester Carter, Sarah Sainsbury, Tom Walter, Joanne Nettleship, Nick Berrow, Ray Owens, Robert Gilbert, Andrew Davidson, Stuart Siddell, Leo L M Poon, Jonathan Diprose, David Alderton, Martin Walsh, Jonathan M Grimes and David I Stuart Affiliations, (2004). The nsp9 replicase protein of SARS-coronavirus, structure and functional insights. PMID: 14962394 PMCID: [PMC7135010](https://www.ncbi.nlm.nih.gov/pmc/articles/PMC7135010/) DOI: [10.1016/j.str.2004.01.016](https://doi.org/10.1016/j.str.2004.01.016) Free PMC article.

43. Trott O and Olsen A. J, (2010). AutoDock Vina: Improving the speed and accuracy of docking with a new scoring function, efficient optimization, and multithreading. *Journal of Computational Chemistry*, 31 (2): 455-461, doi:10.1002/jcc.21334, PMC 3041641, PMID 19499576.
44. Hwang W. C., Lin Y., Santelli E., Sui J., Jaroszewski L., Stec B., Farzan M., Marasco W.A. and Liddington R.C., (2006). Structural basis of neutralization by a human anti-severe acute respiratory syndrome spike protein antibody, 80R. *J Biol Chem* 281: 34610-34616 PubMed: [16954221](https://pubmed.ncbi.nlm.nih.gov/16954221/) Search on PubMed DOI: [10.1074/jbc.M603275200](https://doi.org/10.1074/jbc.M603275200) Primary Citation of Related Structures: [2GHW](#), [2GHV](#).
45. Sutton G., Fry E., Carter L., Sainsbury S., Walter T., Nettleship J., Berrow N., Owens R., Gilbert R., Davidson A., Siddell S., Poon L.L.M., Diprose J., Alderton D., Walsh M., Grimes J. M. and Stuart D. I., (2004). The Nsp9 Replicase Protein of Sars-Coronavirus, Structure and Functional Insights *Structure* 12: 341 PubMed: [14962394](https://pubmed.ncbi.nlm.nih.gov/14962394/) Search on PubMed DOI: [10.1016/j.str.2004.01.016](https://doi.org/10.1016/j.str.2004.01.016) Primary Citation of Related Structures: [1UW7](#).
46. Biedermann F and Schneider H. J., (2016). Experimental binding Energies in Supramolecular Complexes. *Chem. Rev.* 116 (9): 5216-5300. doi: 10.1021/acs.chemrev.5b00583 PMID 27136957.
47. Schalley Christoph A., (March 2012). Introduction (PDF). *Analytical Methods in Supramolecular Chemistry* (2nd ed) Wiley. ISBN 978-3-527-32982-3.
48. Klvana and Martin., (2017). Re: The results from protein-ligand docking shows some unfavourable steric bumps when viewed in Discovery studio.anyone know what does that mean? Retrieved from: https://www.researchgate.net/post/The_results_from_protein-ligand_docking_shows_some_unfavourable_steric_bumps_when_viewed_in_Discovery_studioanyone_know_what_does_that_mean/59e3a932ed99e13e2446c2db/citation/download.
49. Kumar and Rahul., (2017). Re: The results from protein-ligand docking shows some unfavourable steric bumps when viewed in Discovery studio.anyone know what does that mean? Retrieved from: https://www.researchgate.net/post/The_results_from_protein-ligand_docking_shows_some_unfavourable_steric_bumps_when_viewed_in_Discovery_studioanyone_know_what_does_that_mean/59ea0e85cbd5c21d9e40a96d/citation/download.
50. Melesina and Jelena., (2018). Re: Unfavourable bump in molecular docking means the compound is not a good inhibitor?. Retrieved from: <https://www.researchgate.net/post/Unfavourable-bump-in-molecular-docking-means-the-compound-is-not-a-good-inhibitor/5bef65374f3a3e4faf6599d6/citation/download>.
51. Tanuj Sharma, (2017). RE: What is meant by pi-alkyl, pi-pi T shaped and pi-Sulphur interaction in protein-ligand binding? Retrieved from: https://www.researchgate.net/post/What_is_meant_by_pi-alkyl_pi-pi_T_shaped_and_pi-Sulphur_interaction_in_protein-ligand_binding. Oct 12 2017

52. Riley K. E. and Hobza P., (2013). On the importance and Origin of Aromatic Interactions in Chemistry and Biodisciplines. *Acc. Chem. Res.* 46(4): 927-936. doi: 10.1021/ar300083h. PMID 22872015.

53. Korb O., Stürlitzle, T., and Exner, T. E., (2009). Empirical scoring functions for advanced protein-ligand docking with plants. *J Chem Inf Model*, 49(1):84-96.

54. Encyclopædia Britannica, (August 15, 2019). Hydrogen bonding URL:
<https://www.britannica.com/science/hydrogen-bonding>. ACCESS DATE December 07, 2020.

55. Andrews, P. R., Craik, D. J., and Martin, J. L., (1984). Functional group contributions to drug-receptor interactions. *Journal of medicinal chemistry*, 27(12), 1648–1657.
<https://doi.org/10.1021/jm00378a021>.

56. Julie Schaffer (UCD), Corinne Herman (UCD, 2020). Precipitation Reactions Occur when Anions in Aqueous Solution Combine to form an Insoluble ionic solid called a Precipitate.

57. Virtual Chemistry lab, Chemical reactions.
<http://dept.harpercollege.edu/chemistry/chm/100/dgodambe/thedisk/chemrxn/chemrxn.htm>, Retrieved on 25th November, 2020.

58. Ninfa A. J, Ballou D. P, Benore M, eds., (2010). *Fundamental Laboratory Approaches for Biochemistry and Biotechnology*. Dearborn, MI: University of Michigan.

59. Mullis K. B, Faloona F. A., (1987). Specific Synthesis of DNA In Vitro via a Polymerase-catalyzed Chain Reaction. *Methods in Enzymology*. 155 (21): 335–50. doi:[10.1016/0076-6879\(87\)55023-6](https://doi.org/10.1016/0076-6879(87)55023-6). PMID 3431465.